Available online at www.sciencedirect.com

SCIENCE DIRECT®

Lithos 82 (2005) 125–147

LITHOS

www.elsevier.com/locate/lithos

Age of Variscan magmatism from the Balkan sector of the orogen, central Bulgaria

Charles W. Carrigan[a,*], Samuel B. Mukasa[a], Ivan Haydoutov[b], Kristina Kolcheva[c]

[a]*University of Michigan Department of Geological Sciences, Ann Arbor, MI 48109-1063, United States*
[b]*Bulgarian Academy of Sciences, Sofia, Bulgaria*
[c]*Department of Geology and Geography, Sofia University, Sofia, Bulgaria*

Received 31 October 2003; accepted 25 October 2004
Available online 7 April 2005

Abstract

New high-resolution, secondary ion mass spectrometry U–Th–Pb data obtained from zircon and monazite from representative Variscan intrusions in the Balkan sector of the Variscan orogen (Central Bulgaria) constrain the ages of magmatism to the interval ~315–285 Ma. The samples investigated are granitoids from two contrasting intrusive suites. Calc-alkaline granitoids of the first suite include the San Nikola granite (311.9±4.1 Ma) and the Petrohan granodiorite (304.6±4.0 Ma) from the Balkan Terrane, and the Smilovene (304.1±5.5 Ma) and Hisara (303.5±3.3 Ma) granites from the Sredna Gora Terrane. Zircons from these intrusions predominantly lack inherited cores. The second suite consists of two-mica, leucocratic granites and includes the Koprivshtitsa (312.0±5.4 Ma) and Strelcha (289.5±7.8 Ma) plutons. Zircons from intrusions of the second suite are 80–90% xenocrystic. Apparent ages of inherited cores are the magmatic age and slightly older (~300–400 Ma), to Ordovician (~450 Ma) ages, and to Neoproterozoic (~600–900 Ma) ages. Gabbroic magmas related to the first suite are found only in the more northerly Balkan Terrane, while the leucogranites occur only in the southerly Sredna Gora Terrane. Although coeval, the two suites of intrusions are not genetically related, and furthermore were likely derived from different source regions via different melt generating mechanisms. We propose a tectonic and petrogenetic model, whereby following juxtaposition of the Balkan and Sredna Gora Terranes during Variscan collision, the two suites of magmas were generated by continued subduction under eastern Europe due to the influx of mafic magmas into the base of the crust, and by influx of water-rich fluids into high-grade metapsammitic rocks of the Sredna Gora metamorphic series. The new ages are somewhat younger than ages for post-collisional intrusions in the central European Variscan Massifs (i.e., Bohemian, Black Forest, and Vosges), where ages of intrusions are predominantly ~340–320 Ma, although some younger intrusions may also occur. Within the intra-Alpine massifs, both older (~340–320 Ma) and younger (~310–290 Ma) granitoids are present. Farther west, intrusions in the Iberian Massif appear to be predominantly younger ~325–290 Ma, similar to the intrusions of the Balkans. This may indicate that collision of adjacent crustal blocks culminated at earlier times

* Corresponding author. Present address: Olivet Nazarene University, Department of Geology, Bourbonnais, IL 60914, United States.
E-mail address: ccarriga@olivet.edu (C.W. Carrigan).

doi:10.1016/j.lithos.2004.12.010

in the central and more northerly portions of the orogen, and moved both east, west, and south as the evolution of the orogen progressed.

Keywords: Bulgaria; U–Pb geochronology; Zircon; Variscan Orogeny; Granitoids; Balkan; Sredna Gora

1. Introduction

Granitoid magmatism is a significant constituent of most orogenic belts worldwide (e.g., Windley, 1995). Granitic and related rocks serve as windows into the deep crust, shedding light on their source regions and the conditions at the time of magma generation, which in turn can elucidate cryptic deep crustal processes (e.g., Best and Christiansen, 2001). Their ages can be confidently and precisely determined using modern geochronological techniques, and defining their ages serves to pin key geologic events in time based upon the crosscutting relationships of dated components or on correlating features across terranes. Knowledge of their ages, characteristics and distributions is therefore an essential component to understanding orogenic processes and crustal evolution in sufficient detail. Granitoid magmatism plays an especially visible role in the Variscan Orogeny of Europe, where voluminous granitoid magmas occur along with high-grade metamorphic rocks, both compressional and extensional deformation structures, and volcano-sedimentary basins. Ages of granitoids have received considerable attention across western and central Europe, but the ages of similar rocks to the east and southeast remain essentially unknown. The goal of this study is to present new data from the southeastern section of the Variscan orogen in central Bulgaria and discuss the implications of this data set in light of ages determined across the orogen. Our new data are based on an ion microprobe U–Th–Pb study of zircon and monazite from two contrasting suites of granitoid intrusions. Additionally, complementary geochemical data from the literature for these intrusions are synthesized and evaluated in an effort to further elucidate the petrogenetic processes and place constraints upon tectonic scenarios.

The Variscan Orogeny of Europe is correlative to the final stages of the Appalachian orogenies along eastern North America, and marks the final amalgamation of Laurasia and Gondwana to form the supercontinent Pangea. Within Europe, basement terranes form a collage of blocks with both continental and oceanic affinities (Matte, 1986; Ziegler, 1986; Matte, 1991). Throughout the Paleozoic, the northern (i.e., Baltica and Laurentia) and southern (Gondwana) continents interacted through a series of rifting and collisional events involving island arcs, rifted continental fragments, and the major continents. Various terranes of Gondwanan affinity drifted northward across the paleo-oceans that existed between Gondwana and Laurasia, and collided with both Laurentia and Baltica beginning with the accretion of Avalonia during the Ordovician–Silurian (Van der Voo, 1988; Tait et al., 1997; McKerrow et al., 2000; Tait et al., 2000; Winchester et al., 2002). Although the existence of Pangea is universally accepted, the identities and geometries of the final colliding blocks with southern Europe are debated (e.g., Stampfli and Borel, 2002; Muttoni et al., 2003). Numerous massifs within Europe expose Variscan rocks, and include the Bohemian, Odenwald, Black Forest (Schwarzwald), Vosges, Massif Central, and Iberian massifs. Within the Alpine Orogeny, smaller, isolated massifs also occur from the western Alps, to the northern Carpathians and to the southerly Balkanides (Fig. 1).

2. Variscan geology of Bulgaria

2.1. Tectonic terranes in central Bulgaria related to the Variscan Orogeny

Four principal terranes occurring in Bulgaria and surrounding countries (from north to south: Moesian, Balkan, Sredna Gora, and Rhodope) expose Variscan-age rocks and were likely involved in the Variscan Orogeny of southeastern Europe (Fig. 1; Haydoutov and Yanev, 1997; Yanev, 2000). The Balkan and Sredna Gora Terranes comprise the basement into which the studied Variscan granitoids intruded.

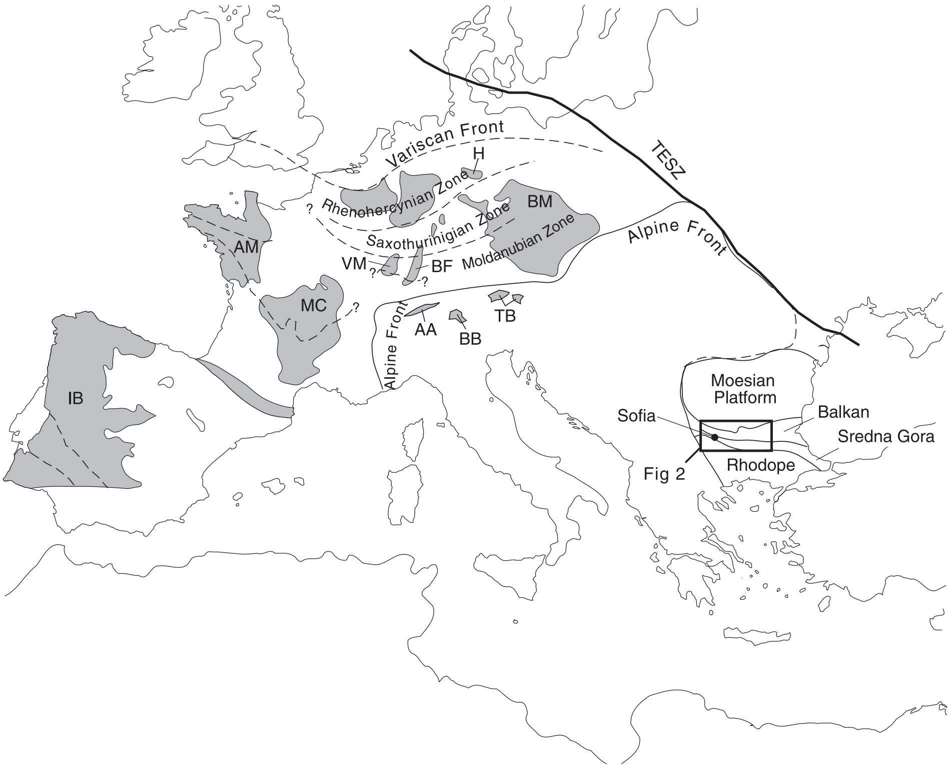

Fig. 1. Simplified geologic map of European Variscan Massifs. IB=Iberian Massif, AM=Armorica Massif, MC=Massif Central, VM=Vosges Massif, BF=Black Forest Massif, AA=Aar Batholith, BB=Bernina Batholith, TB=Tauern Batholith, BM=Bohemian Massif, H=Harz Massif, TESZ=Trans European Suture Zone.

Effects of the younger Alpine deformational and metamorphic events–Cretaceous to Tertiary in age–are largely concentrated in the southernmost Rhodope Terrane, and are limited to large open folds and discrete shear zones in the more northerly terranes (Haydoutov, 1989).

The Moesian platform consists of silicic low- to high-grade metamorphic rocks of Neo- and Paleo-Proterozoic age, low-grade metamorphic Neoproterozoic–Cambrian turbidites, and Paleozoic sedimentary rocks (Sãndulescu, 1994; Haydoutov and Yanev, 1997; Seghedi et al., 1999). The Balkan Terrane, immediately to the south, is floored by a Neoproterozoic ophiolite and a Cambro–Ordovician island arc (Kalenic, 1966; Lilov, 1981; Haydoutov, 1989; von Quadt et al., 1998; Savov et al., 2001), both of which may have correlatives in the Bohemian Massif to the NW and several massifs in Turkey and the Arabian Peninsula to the SE. The ophiolite and island arc rocks are overlain by a low-grade Lower Ordovician olistostrome (Arenigian; Kalvacheva, 1986) composed primarily of rocks derived from the ophiolite and island arc, suggesting obduction of this terrane at this time. The overlying unmetamorphosed Paleozoic sedimentary rocks include Upper Ordovician glacial diamictite deposits, Silurian argillites, Middle Devonian to Lower Carboniferous flysch sediments, and Upper Carboniferous to Permian molasse (Haydoutov and Yanev, 1997). Differences in the Paleozoic stratigraphy of the Balkan and Moesian Terranes suggest separate evolution in the Early to Middle Paleozoic, culminating with their juxtaposition during the Variscan Orogeny in the Late Carboniferous (Haydoutov and Yanev, 1997; Yanev, 2000). Paleogeographic data (lithostratigraphy, biostratigraphy and sparse paleomagnetism) all indicate a Gondwanan affinity for the Balkan Terrane and that it migrated northward during the Paleozoic, similar to other tectonic blocks of Gondwanan affinity found in southern Europe (Haydoutov and Yanev, 1997; Yanev, 2000). Similarly, lithostratigraphic, biostratigraphic and paleomagnetic data indicate a European affinity during the Middle Triassic (Muttoni et al., 2000 and references therein), further supporting the notion of accretion to southern Baltica during the Variscan Orogeny. Haydoutov and Yanev (1997) also postulated a correlation between the Moesian/Balkan Terranes with the Bohemian Massif. They further state that it comprises the missing link between the Avalonian–Cadomian and Arabian peripheral orogens of Gondwana (Nance and Murphy, 1994).

Based on field relations and rock fabrics, the oldest rocks of the Sredna Gora Terrane are high-grade metamorphic rocks that have received little study so far. Metapsammites predominate, although metapelites, garnet amphibolites, eclogites, and orthogneisses are present as well (Zagorchev et al., 1973). The metamorphic grade of most rocks is in the upper amphibolite facies, but the presence of eclogites (Dimitrova and Belmustakova, 1982a,b), which are in all likelihood much higher-pressure rocks than the rest of the metamorphic basement, suggests that the basement may be a composite terrane. The age of metamorphism in the basement is Variscan (~335 Ma, Carrigan unpub. data in prep.), and late Variscan granitoids intrude the high-grade basement rocks (Zagorchev et al., 1973).

The Rhodope massif straddles the Bulgarian and Greek border south of the Sredna Gora Terrane, and consists of a complexly metamorphosed high-grade assemblage of dismembered ophiolites, metagabbros, felsic orthogneisses, amphibolites, metapelites, carbonates, and eclogites (Papanikolaou and Panagopoulos, 1981; Kozhoukharova, 1985; Mposkos, 1989; Kozhoukharov, 1987; Burg et al., 1990; Liati and Mposkos, 1990; Kozhoukharova, 1996). Contacts in the Rhodope Terrane are commonly highly sheared, often making geologic field interpretations equivocal. Unlike the more northerly terranes, the Rhodope massif underwent high-grade Alpine metamorphism and intense deformation during the Eocene (Arnaudov et al., 1990; Liati and Gebauer, 1999) and Cretaceous (Wawrzenitz and Mposkos, 1997), and its pre-Alpine history is therefore obscured. However, evidence for its pre-Alpine history is becoming available and recent dating of orthogneisses by U–Pb zircon methods yield late Variscan ages in the range of ~320–290 Ma (Peytcheva and von Quadt, 1995, 319±9 Ma, 305±52 Ma; Liati and Gebauer, 1999, 294±8 Ma; Peytcheva et al., 2000, ~300 Ma; Cherneva et al., 2002, 311.1±4.3 Ma; Carrigan et al., 2003b, 301±4 Ma). These ages are strikingly similar to the ages of unmetamorphosed and undeformed granites of the Balkan and Sredna Gora Terranes reported in this study, and this suggests that parts of the Rhodope Terrane were involved in the Variscan Orogeny.

2.2. Previous work on Variscan granitoids in Bulgaria

2.2.1. Granitoids in the Balkan Terrane

Variscan granitoids in the Balkan Terrane are best exposed in the Stara Planina intrusive complex, an east–west elongate body in the central part of the terrane. These rocks range in composition from mafic to intermediate to felsic and follow typical calc-alkaline geochemical trends (Haydoutov, 1991; Fig. 2). Granites are commonly biotite bearing and some contain megacrystic feldspar. More mafic varieties containing hornblende also occur and gabbros are also present in small amounts. Minor minerals commonly include titanite, apatite, opaques, zircon, and secondary epidote and muscovite. Major element geochemical data from Haydoutov (1991) for the representative San Nikola granitoid indicate a range of SiO_2 (60–67 wt.%), moderate FeO (3–5 wt.%), low Fe# (atomic $Fe^{2+}/(Mg+Fe^{2+})$; ~0.5–0.7), calcic to calc-alkalic compositions, K_2O/Na_2O ratios ~0.7–1.2, and metaluminous to weakly peraluminous compositions (based on aluminum saturation index, ASI=molecular Al/Na+K+2(Ca–5/3P); ~0.9–1.1). The more mafic Petrohan granodiorite follows similar geochemical trends for major oxides, with SiO_2 (53–59 wt.%), high FeO (6.5–8.5 wt.%), low Fe# (~0.5), calcic composition, K_2O/Na_2O ratios ~0.5–0.7, and metaluminous compositions (ASI~0.75–0.85). Related volcanic rocks are also common in the Balkan Terrane, where they are associated with Upper Paleozoic molasse sediments (Haydoutov, 1991). Few geochronological studies have been done on these rocks, but recent data for the Vejen pluton yielded an age of 314±4.8 Ma (Kamenov et al., 2002).

2.2.2. Granitoids in the Sredna Gora Terrane

Previous workers divided the granitoids of the Sredna Gora Terrane into three suites of magma

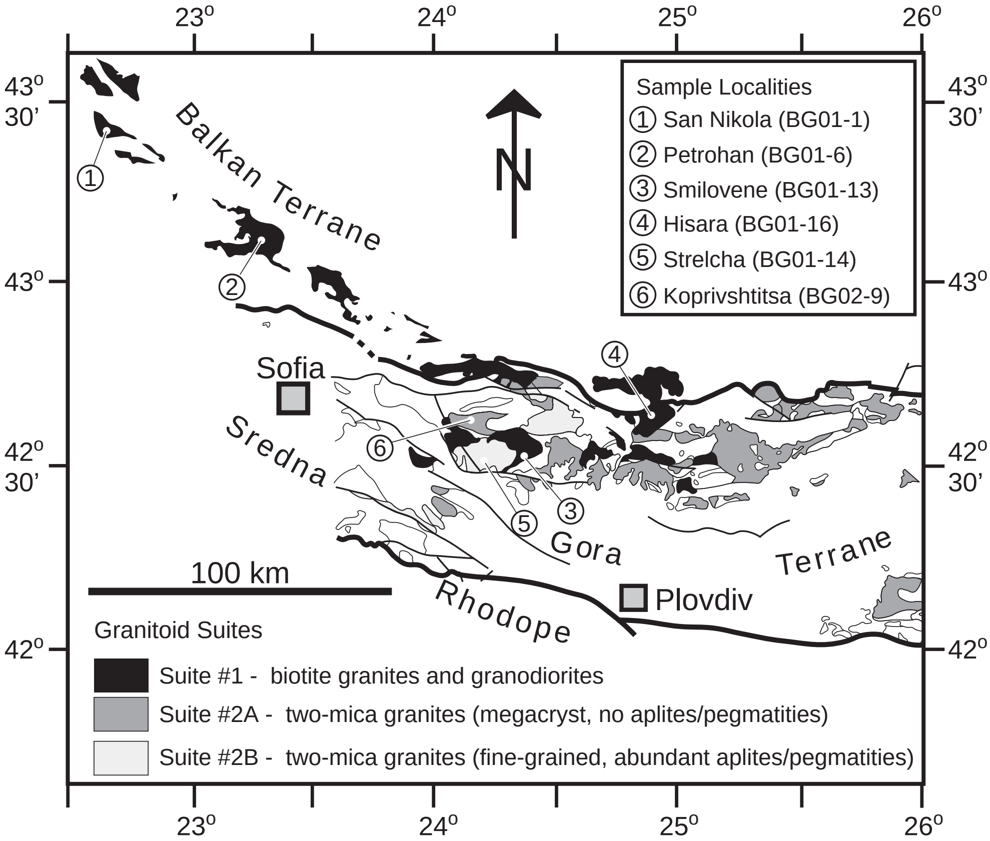

Fig. 2. Simplified geologic map of Variscan granitoids in the Balkan and Sredna Gora Terranes of central Bulgaria.

emplacement based upon field relations, modal mineralogy, grain size, and the presence or absence of aplites and/or pegmatites (Zagorchev et al., 1973; Fig. 2). The first and presumably oldest intrusive suite consists primarily of biotite-bearing granites, hornblende-bearing granodiorites and some quartz diorites. Whole-rock major element geochemistry from Ruseva (1978) and Moorbath and Zagorchev (1983) for the representative Smilovene and Hisara granitoids indicate a range of SiO_2 (~60–72 wt.%), moderate FeO (5–1 wt.%), low Fe# (~0.4–0.75), calcic to calc-alkalic compositions, K_2O/Na_2O ratios ~0.6–0.9 and metaluminous to weakly peraluminous compositions (ASI~1.0–1.1). Granitoids of this suite are strikingly similar to the granitoids to the north in the Balkan Terrane (e.g., compare data for Smilovene and San Nikola granites) in their mineralogy and geochemistry. Rb–Sr whole-rock isochrons for the Smilovene and Hisara intrusions yielded ages of 342±27 and 338±9 Ma with initial $^{87}Sr/^{86}Sr$ ratios of 0.7060 and 0.7054, respectively (Moorbath and Zagorchev, 1983). Sr concentrations are surprisingly low (~100 ppm) for rocks of this type and Rb/Sr ratios range from ~0.3 to 1 (Moorbath and Zagorchev, 1983; Boyadjiev, 1991). Trace element data of Boyadjiev (1991) show chondrite-normalized rare earth element (REE) patterns of ~30–130 times enrichment for light rare earth elements (LREE), ~6–12 times enrichment for heavy rare earth elements (HREE), and slight negative Eu anomalies. Concentration data for Ta, Yb, and Rb (Boyadjiev, 1991) plot on tectonic discrimination diagrams of Pearce et al. (1984) as "volcanic arc granites". Zr concentrations are also surprisingly low for granitic rocks (~60 ppm) and yield zircon saturation temperatures (T_{Zr}, Watson and Harrison, 1983) in the range of 690–740 °C.

The second and third intrusive suites consist of strongly peraluminous, two-mica, leucocratic granites. Based on the strong similarities between the granites of the second and third intrusive suites, we combine the two-mica granites into suites 2A and 2B, equivalent to the second and third intrusive suites of Zagorchev et al. (1973). Other phases commonly present include garnet, apatite, zircon, and monazite. Samples of suite 2A typically contain megacrystic feldspars and lack associated aplites and pegmatites, while suite 2B is associated with abundant aplites and pegmatites and displays a finer-grained, uniform texture. These distinctions, however, may have little to do with the petrogenesis of the rocks. Major element geochemical data from Ruseva (1978) for the Koprivshtitsa and Strelcha granites show strong similarities between the different two-mica granites, and compared to the first complex they are much more enriched and restricted in SiO_2 (~70–75 wt.%), lower in FeO (~2.0–0.2 wt.%), have similarly low Fe # (~0.4–0.7), are slightly more alkalic, have similar K_2O/Na_2O ratios (~0.6–1.1), and have weakly to strongly peraluminous compositions (ASI~1.1–1.4). Rb–Sr whole-rock isochron data yielded ages of 320±58 Ma and 301±7 Ma for the Koprivshtitsa granite (suite 2A), and 271±26 Ma and 238±37 Ma for the St. Georgi and Strelcha plutons, respectively (suite 2B); initial $^{87}Sr/^{86}Sr$ isotopic ratios for both groups of two-mica granites are similar and fall in the range of ~0.7090–0.7096 (Zagorchev and Moorbath, 1986). Trace element data from Boyadjiev (1991) indicate notably higher Sr concentrations for the Koprivshtitsa (~300 ppm) and Strelcha (~390 ppm) plutons (suites 2A and 2B, respectively) compared with the first suite (~100 ppm). Chondrite-normalized REE patterns for suites 2A and 2B differ somewhat (~30–40× and ~50–115× enrichment in LREE, ~8–9× and ~3–8× enrichment in HREE, respectively, both with negative Eu anomalies), but the patterns between all suites are similar. Similarly, data for Ta, Yb and Rb also plot in tectonic discrimination diagrams of Pearce et al. (1984) as "volcanic arc granites". Zr concentrations are again anomalously low for granitic rocks (~10–45 ppm; Boyadjiev, 1991), and yield unrealistic zircon saturation temperatures in the range of 600–690 °C.

The Rb–Sr ages suggest a wide span of intrusive events covering ~100 million years and also suggest that the suites are distinct in age. The Middle Triassic age for the Strelcha pluton is much younger than Variscan events; this age has more in common with the Triassic Cimmerian event of southern Asia (Şengör, 1987) than with the Variscan Orogeny of Europe. The new data below, however, allow a significant revision of the ages of these three intrusive suites. Similar reassessments may be warranted for published isotopic age information in other granitoid belts of the Variscan Orogen.

3. Methods of data collection and interpretation

Zircon and monazite were separated using standard mineral separation techniques from approximately 3 to 10 kg of fresh, representative samples. Approximately 40–50 grains from each sample were mounted in epoxy with fragments of zircon standards AS3 (1099.1±0.5 Ma; Paces and Miller, 1993; Schmitz et al., 2003) and 91500 (81.2 ppm U; Wiedenbeck et al., 1995), or monazite standard 554 (45±1 Ma; Harrison et al., 1999), and polished to their approximate centers. Grains were imaged with back-scattered electron (BSE) and/or cathodoluminescence (CL) imaging techniques using the Hitachi Scanning Electron Microscope and/or the Cameca SX-100 Electron Microprobe, both housed at the University of Michigan Electron Microbeam Analysis Laboratory. Grain images were used as guides for selecting spots for analysis. Grain mounts were washed with a dilute acid (~0.5 N HCl) in an ultrasonic bath for ~10 min prior to gold coating to remove surface common Pb contamination. Additionally, analytical spots were pre-sputtered with the O^- primary ion beam for 180 s prior to analysis. Zircon and monazite were analyzed for isotopic composition of U, Th and Pb by high-resolution, secondary ion mass spectrometry (HR-SIMS) using the Cameca IMS-1270 ion microprobe at the W.M. Keck Foundation Center for Isotope Geochemistry National Ion Microprobe Facility, University of California, Los Angeles. Ion microprobe operational techniques are highly standardized, and follow those described in Harrison et al. (1995) and Quidelleur et al. (1997). The largest source of error in HR-SIMS U–Th–Pb dating results from the calibration of the standardization curve; information on the standard curves used in this study is available from the first author (CWC), and all data presented include calibration errors. After a working standard curve was established, standards were analyzed approximately every four unknowns. $^{206}Pb/^{204}Pb$ ratios for zircon analyses are nearly all >1000; about half are over 10,000, indicating very high percentages of radiogenic Pb and very small to insignificant common Pb corrections. Similarly, $^{208}Pb/^{204}Pb$ ratios from monazite analyses are nearly all >4500. Common Pb in zircon was corrected using either a ^{204}Pb or ^{208}Pb correction depending upon sample $^{207}Pb/^{204}Pb$ and $^{208}Pb/^{204}Pb$. Analyses with low $^{207}Pb/^{204}Pb$ and $^{208}Pb/^{204}Pb$ (<200) are often reversely discordant, and typically require a ^{208}Pb correction to eliminate reverse discordance. Monazite common Pb was corrected using ^{204}Pb. Common Pb compositions were estimated using a Stacey-Kramers model Pb isotopic composition (Stacey and Kramers, 1975) at 300 Ma.

Spot selection and data analysis were performed similar to the methods described in Miller et al. (2000) and Carrigan et al. (2003a). Ages were interpreted in light of zoning patterns. We interpret outermost, euhedral, concentric, oscillatory zones as representing magmatic growth, while interior zones with truncations and either homogeneous, patchy or euhedral zoning we interpret as inherited cores (Paterson et al., 1989; Vavra, 1990; Miller et al., 1992; Hanchar and Miller, 1993). U–Th–Pb analyses of these respective zones can serve to supplement these interpretations; zones interpreted as magmatic should all yield the same age (while taking into account the possibility of partial Pb loss) as well as similar Th/U ratios. Conversely, inherited grains will not show the same consistencies in ages or in actinide geochemistry, but rather should exhibit a large scattering of information (except in the unlikely event that all inherited grains are of the same population). Ablated grains were re-imaged using BSE and reflected light to determine exact spot locations.

Analyses from magmatic zones were pooled for each sample to calculate the sample age using the ISOPLOT concordia age described by Ludwig (1991, 1998). With few exceptions, a large pool of analyses does not constitute a single X–Y weighted mean with a reasonable MSWD, and outliers must be removed for proper age calculations. Suites of analyses typically consist of an upper cluster (likely representing the true age) and variable spread downward to younger ages. Young, statistical outliers (based upon weighted residuals), presumably reflecting partial Pb loss, are excluded and the age and MSWD recalculated until acceptable values (MSWD of equivalence and MSWD of concordance <2.0) are obtained (e.g., Miller et al., 2000; Carrigan et al., 2003a). However, a few analyses are reversely discordant and have $^{206}Pb^*/^{238}U$ ages that are older than the rest of the sample population. These cannot be removed based upon an assumption of Pb loss, but clearly are the cause of poor statistical parameters. Such anomalous analyses are also occasionally observed when analyses of standards are plotted against their own calibration curve, suggesting that some analyses are not well described by the calibration. Therefore, in a few cases, we removed analyses that are both reversely discordant and slightly older than the rest of the population and were causing unacceptable statistical parameters. Inherited cores were analyzed as operational time allowed and are treated individually.

Additionally, we analyzed the data for the strongest probability of concordance (most likely representing the true age) by plotting them on concordia probability plots, which are the intersection of the concordia curve with the summed Gaussian joint density function in bivariate U–Pb space (Carrigan et al., 2003a). Probability plots along concordia give more weight to analyses with smaller analytical errors and a higher degree of concordance, and consider multiple U–Pb age information simultaneously compared to simpler probability plots based only on $^{206}Pb^*/^{238}U$ or $^{207}Pb^*/^{206}Pb^*$ ages. The two methods of age determination employed here (pooled X–Y weighted mean and the peak position of the probability curve) yield very similar ages. Uncertainties in tables, text and figures are shown at the 95% confidence interval, and calculated pooled ages include errors in the calibration curves and U decay constants. Representative BSE/CL images for the calc-alkaline and strongly peraluminous granitoid suites are presented in Figs. 3 and 4, respectively. U–Pb zircon data for analyzed spots are presented in Figs. 5–7 and in Table 1.

Analyses of monazite standard 554 commonly yield a large spread along the calibration plot (M. Grove, UCLA, pers. comm.), and the standard data acquired in this study cluster in two groups at ThO_2/Th values of ~2.8–3.0 and ~0.7–0.8. The unknowns all have ThO_2/Th values close to the upper cluster, but

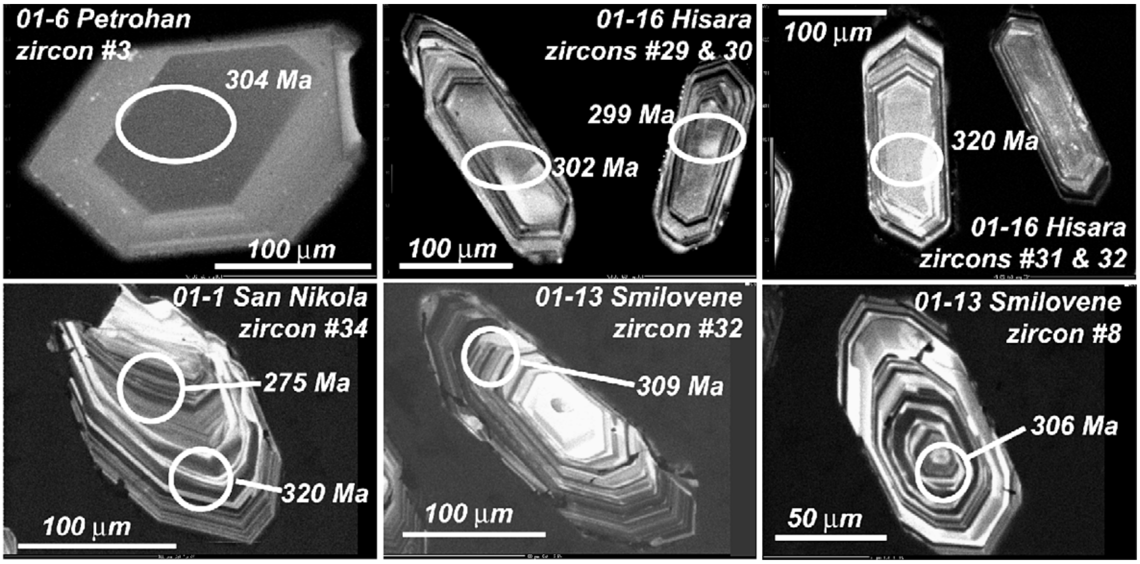

Fig. 3. Cathodoluminescence images of representative zircon grains for the calc-alkaline granitoids (suite 1; samples 01-1, 01-6, 01-13 and 01-16). All have well-developed, euhedral, oscillatory zoning from core to rim; inherited cores are sparse or completely absent. Individual spots shown are $^{206}Pb^{*}/^{238}U$ ages.

including the lower cluster in the calibration curve greatly improves the precision of the ages of the unknowns. If the standard analyses of the lower cluster are removed from the standard calibration, the errors on the individual analyses increase by a factor of ~4–8, but the means are essentially unaffected. Additionally, the differences in the errors do not significantly affect the geological interpretations; therefore, the data

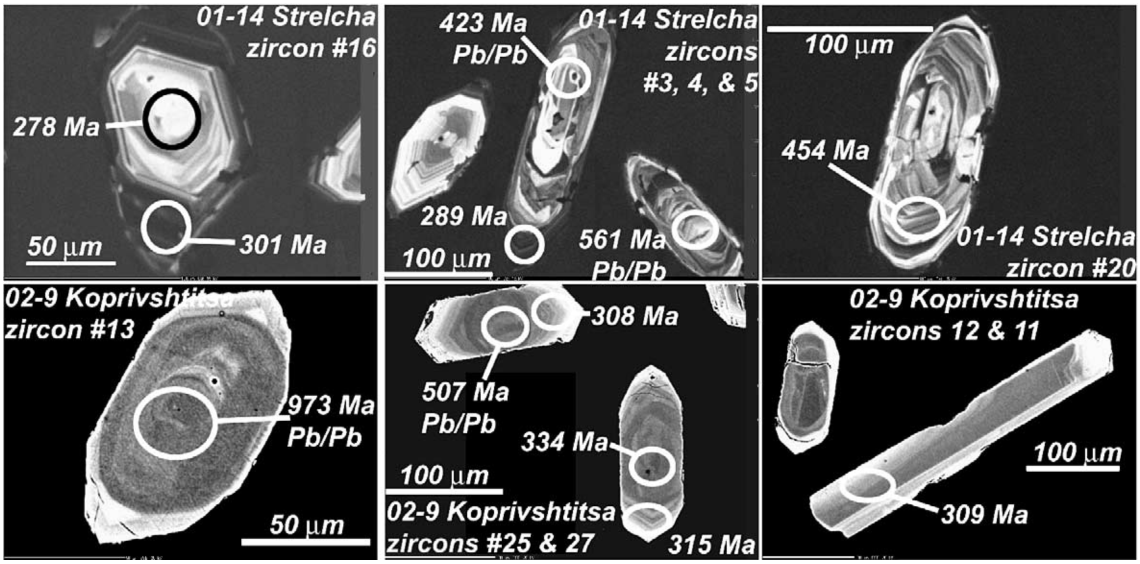

Fig. 4. Back-scattered electron (sample 02-9) and cathodoluminescence (sample 01-14) images of representative zircon grains for the two-mica granites (suite 2). Grains are ~80–90% xenocrystic (inherited cores), with very thin, bright (in BSE; very dark in CL), magmatic rims. Zoning of inherited cores varies from magmatic to patchy to homogeneous. Ages of individual spots shown are $^{206}Pb^{*}/^{238}U$ unless indicated as Pb/Pb ($^{207}Pb^{*}/^{206}Pb^{*}$).

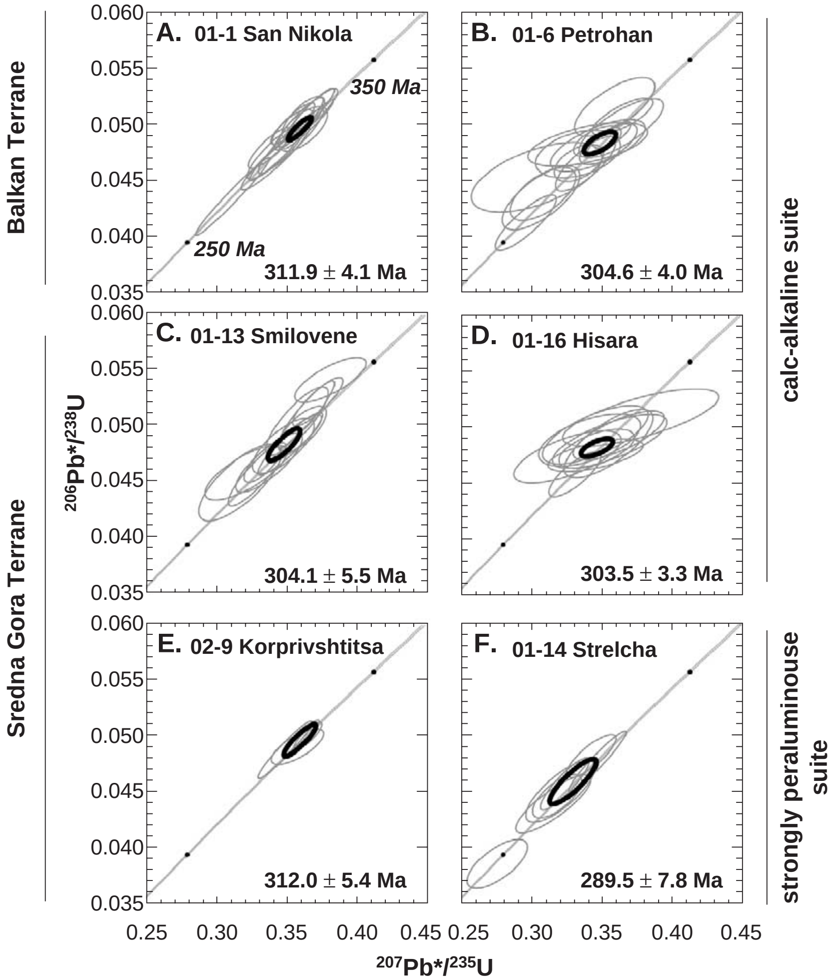

Fig. 5. Concordia plots of zircon U–Pb data showing magmatic ages. Scale ranges are identical for comparison. Analyses are dark gray lines; thick black lines are concordia age error ellipses. One significantly younger point for samples 01-13 and 01-14 not shown.

reported here include the lower cluster of standard analyses in the Th–Pb calibration. BSE images of representative monazite grains from sample 02-9 are presented in Fig. 8. New monazite Th–Pb data are presented in Fig. 9 and Table 2. Preferred pooled ages for the studied samples are listed in Table 3.

4. Sample descriptions and results

4.1. Balkan Terrane

We sampled two representative intrusions in the Balkan Terrane, the San Nikola granite (BG01-1) and the Petrohan granodiorite (BG01-6). Zircons from both samples are prismatic, euhedral grains that display concentric, euhedral zoning throughout (Fig. 3). A few sparse cores appear to be present in CL images of the San Nikola sample and are typically dominated by strong oscillatory zoning. However, they yield similar ages to the rims and cannot be distinguished by our data. They may represent complex magma chamber or lower crustal processes occurring during the melting event. Inherited cores are entirely absent in the Petrohan sample.

The 14 analyses of San Nikola zircons (BG01-1) yield ages between 275 Ma and 321 Ma. The spread

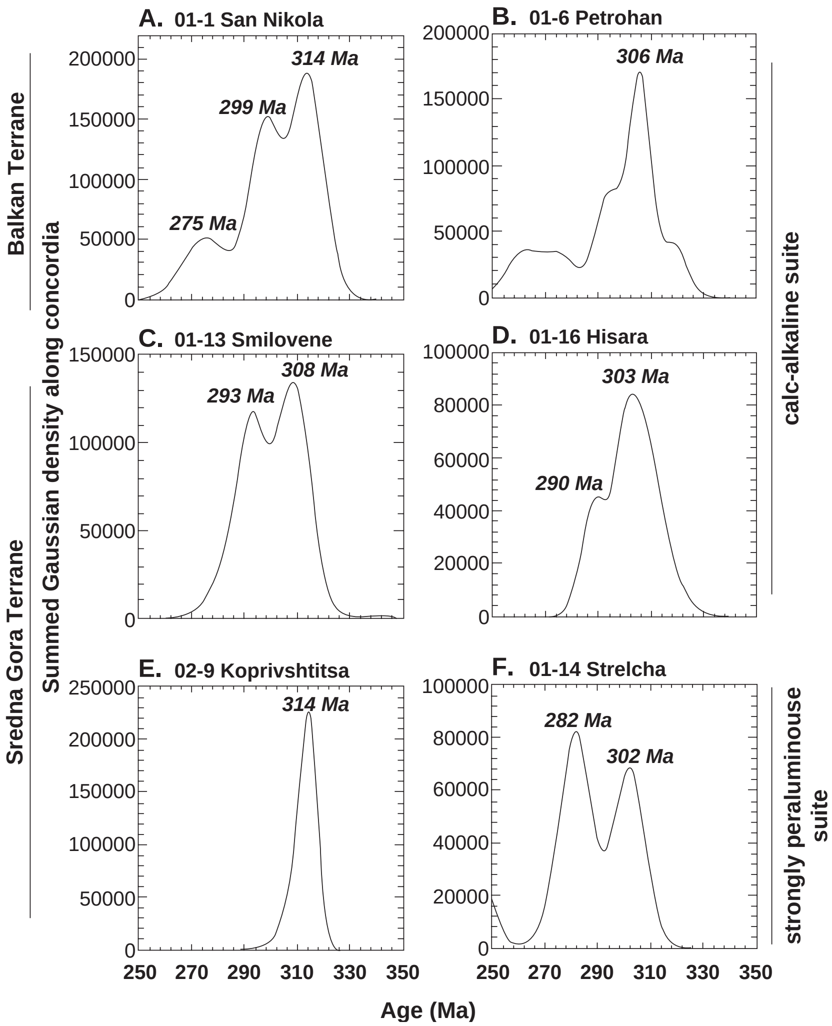

Fig. 6. Concordia probability plots (after Carrigan et al., 2003a) for magmatic ages calculated using $^{206}Pb^{*}/^{238}U$ and $^{207}Pb^{*}/^{235}U$ data simultaneously. The plots are the intersection of the concordia curve with the Gaussian joint density function in bivariate U–Pb space, summed for all analyses. Analyses with smaller analytical errors and a higher degree of concordance are more influential on the position of the peak of the curve. Age scales (x-axes) are identical for comparison.

in the data is entirely consistent with an older peak that represents the true age and spread downward to younger ages due to partial Pb loss. Two analyses (34_sp2, 31_sp1) are interpreted as representing partial Pb loss. Two analyses (5_sp1, 6_sp1) are reversely discordant and result in poor statistical parameters of the calculated age. The remaining analyses yield a concordia age of 311.9±4.1 Ma (MSWD equiv.=1.4, MSWD conc.=1.4, n=10; Fig. 5A) that we accept as the best approximation to the true age. The probability plot along concordia yields three peaks at 275 Ma, 299 Ma, and the highest at 314 Ma (Fig. 6A). U concentrations range from ~380 to ~1300 ppm U. Th/U ratios range from 0.26 to 0.57, with one outlier at 0.91.

Analyses of zircons from the Petrohan granodiorite (BG01-6) range in age from ~260 Ma to ~320 Ma. Four analyses (7_sp1, 22_sp1, 24_sp1 and 30_sp1) are younger than the rest of the population and contribute to a separate, younger peak on the probability plot at ~270 Ma (Fig. 6B). These are interpreted as representing partial Pb loss. Another

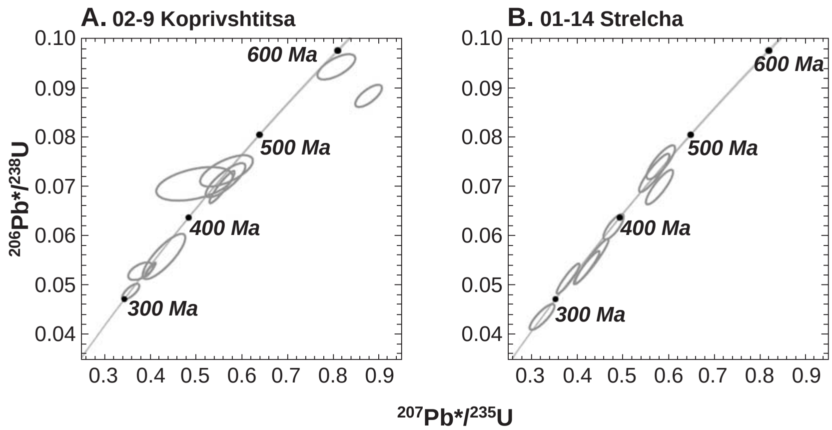

Fig. 7. Concordia plots of zircon U–Pb data for inherited cores in two-mica granites. Both samples contain a subpopulation of Early Carboniferous–Devonian (~340–400 Ma), Ordovician (~450 Ma) and Neoproterozoic (~600–900 Ma) ages.

analysis (25_sp1) is slightly older than the rest of the population and reversely discordant, and may represent a calibration error. The remaining analyses yield a concordia age of 304.6±4.0 Ma (MSWD equiv.=1.8, MSWD conc.=1.18, n=10; Fig. 5B). The probability plot along concordia also yields a distinct peak at 306 Ma (Fig. 6B). U concentrations scatter from ~130 to ~620 ppm, but most analyses cluster between ~130 and 350 ppm U. Th/U ratios are very consistent and all but one analysis lie in the range ~0.9–1.1.

4.2. Sredna Gora Terrane

4.2.1. Biotite-bearing granites of the first suite

Two samples of biotite-bearing granites in the Sredna Gora Terrane were obtained for geochronology, the Smilovene (BG01-13) and the Hisara (BG01-16) plutons. Zircons from both samples are prismatic, euhedral grains that display concentric, euhedral zoning. Inherited cores are sparse, but where analyzed yield ages indistinguishable from the remaining data points, similar to the samples from the Balkan Terrane (Fig. 3).

The 14 analyses of the Smilovene granite (BG01-13) yield a spread of ages between ~290 Ma and 340 Ma, with one much younger analysis at ~170 Ma (4_sp1) interpreted as Pb loss. The two oldest analyses (18_sp1, 22_sp1) extend away from the rest of the population, are strongly reversely discordant and are interpreted to reflect a calibration error. Three additional young data points, causing excess scatter in the data, were removed on an assumption of partial Pb loss (7_sp1, 25_sp1, 35_sp1). The remaining data yield a concordia age of 304.1±5.5 Ma (MSWD equiv.=1.8, MSWD conc.=2.3, n=8; Fig. 5C). The probability plot along concordia yields a slightly older peak at 308 Ma (Fig. 6C). Although the MSWD of concordance is slightly high, we judge that removing additional data points is too arbitrary. U concentrations predominantly range from ~320 to ~990 with one analysis much higher at ~1670 ppm U; Th/U ratios range from 0.29 to 0.72.

All analyses of the Hisara granite (BG01-16) yield a concordia age of 303.5±3.3 Ma (MSWD of equiv.=1.4, MSWD conc.=0.82, n=10; Fig. 5D), and the probability plot along concordia yields a comparable peak at 303 Ma (Fig. 6D). U concentrations range from ~325 to 510 ppm U, with one analysis at a higher value of ~650 ppm U. Th/U ratios range from 0.31 to 0.56.

4.2.2. Two-mica granites of the second suite

4.2.2.1. Zircon ages. Zircons from the two-mica granites are strikingly different from those of the calc-alkaline suite. In contrast to the purely magmatic grains in the biotite-bearing granitoids, roughly 80–90% of the zircon grains in the two-mica granites are xenocrystic with thin, euhedral, bright (in BSE) magmatic rims (Fig. 4). The magmatic rims are not always continuous around the inherited cores, and some grains have only small hints of new growth

Table 1
High resolution, secondary ion mass spectrometry U–Pb zircon data for analyzed spots

Analysis[a]	Isotopic ratios					Calculated ages						U conc.	Th/U	^{206}Pb/^{204}Pb	^{207}Pb/^{204}Pb	^{208}Pb/^{204}Pb
	^{206}Pb*/^{238}U	2σ	^{207}Pb*/^{235}U	2σ	Correlation coefficient	^{206}Pb*/^{238}U	2σ	^{207}Pb*/^{235}U	2σ	^{207}Pb*/^{206}Pb*	2σ					
01-1_3_sp1*	0.0470	0.0023	0.3417	0.0197	0.9409	296.4	14.2	298.5	14.9	315.1	46.0	733	0.91	23,261	1224	6751
01-1_4_sp1*	0.0512	0.0017	0.3693	0.0135	0.8815	321.7	10.3	319.1	10.0	300.1	39.4	799	0.26	29,388	1543	2448
01-1_5_sp1	0.0479	0.0015	0.3378	0.0126	0.8473	301.9	9.2	295.5	9.6	245.6	45.6	473	0.51	15,292	802	2479
01-1_7_sp1*	0.0496	0.0016	0.3614	0.0143	0.6599	312.4	9.9	313.3	10.6	320.1	69.0	377	0.33	13,691	730	1474
01-1_6_sp1	0.0501	0.0015	0.3541	0.0127	0.8767	315.2	9.2	307.8	9.6	252.1	40.0	554	0.35	18,291	960	2045
01-1_12_sp1*	0.0497	0.0013	0.3541	0.0118	0.7209	312.8	8.3	307.8	8.8	269.8	53.4	672	0.47	11,769	622	1917
01-1_16_sp1*	0.0506	0.0016	0.3615	0.0124	0.7470	318.4	9.5	313.3	9.3	275.9	53.6	639	0.40	14,692	778	1989
01-1_19_sp1*	0.0500	0.0018	0.3652	0.0146	0.9597	314.8	10.8	316.1	10.9	326.0	26.6	1188	0.57	73,694	3927	14050
01-1_23_sp1*	0.0501	0.0019	0.3585	0.0141	0.9109	315.2	11.6	311.1	10.5	280.7	37.4	788	0.34	33,010	1718	3439
01-1_23_sp2*	0.0477	0.0021	0.3429	0.0174	0.8849	300.4	12.7	299.3	13.1	291.4	54.0	848	0.41	23,473	1244	3038
01-1_24_sp1*	0.0486	0.0023	0.3528	0.0190	0.9276	305.6	14.4	306.8	14.2	316.2	45.8	666	0.36	93,960	4889	10510
01-1_34_sp1*	0.0509	0.0019	0.3658	0.0146	0.9317	320.0	11.9	316.5	10.9	291.5	33.2	1111	0.46	130,510	6787	19050
01-1_34_sp2	0.0436	0.0028	0.3113	0.0216	0.9784	275.2	17.4	275.2	16.7	274.9	33.6	1039	0.29	45,044	2384	4084
01-1_31_sp1	0.0471	0.0017	0.3411	0.0148	0.9479	297.0	10.7	298.0	11.2	305.9	33.0	1309	0.56	33,139	1746	5965
01-13_4_sp1	0.0265	0.0013	0.1979	0.0175	0.6780	168.5	8.0	183.4	14.9	379.5	149.0	1674	0.45	1689	105	292
01-13_6_sp1*	0.0512	0.0024	0.3635	0.0166	0.9226	321.6	14.9	314.8	12.3	264.6	42.2	988	0.56	20,729	1073	3660
01-13_7_sp1	0.0460	0.0020	0.3209	0.0238	0.7510	289.8	12.3	282.6	18.3	223.7	116.8	318	0.53	7099	381	1170
01-13_8_sp1*	0.0485	0.0023	0.3523	0.0188	0.9210	305.5	14.0	306.5	14.1	313.9	47.6	817	0.72	19,931	1057	4623
01-13_9_sp1*	0.0498	0.0017	0.3608	0.0141	0.7184	313.3	10.4	312.8	10.5	309.0	63.2	294	0.56	22,433	1160	4136
01-13_10_sp1*	0.0468	0.0014	0.3328	0.0108	0.7591	294.8	8.4	291.7	8.2	267.5	49.4	596	0.53	12,390	651	2108
01-13_11_sp1*	0.0468	0.0021	0.3373	0.0193	0.8228	295.1	13.2	295.1	14.6	295.1	74.2	391	0.67	16,019	836	3293
01-13_18_sp1	0.0542	0.0016	0.3808	0.0206	0.7498	340.3	9.9	327.6	15.2	238.8	86.2	384	0.37	10,669	548	1272
01-13_22_sp1	0.0523	0.0018	0.3718	0.0146	0.8626	328.4	10.8	321.0	10.8	267.5	45.4	831	0.45	10,082	535	1466
01-13_24_sp1*	0.0505	0.0025	0.3571	0.0181	0.8279	317.9	15.3	310.1	13.6	251.9	67.6	763	0.29	17,590	893	1632
01-13_25_sp1	0.0458	0.0023	0.3287	0.0167	0.8821	288.7	14.1	288.6	12.8	287.6	56.0	413	0.47	21,752	1127	3132
01-13_27_sp1*	0.0483	0.0020	0.3473	0.0179	0.7363	304.2	12.3	302.7	13.5	290.5	80.2	430	0.43	13,039	711	1872
01-13_32_sp1*	0.0490	0.0017	0.3555	0.0156	0.8649	308.5	10.4	308.8	11.7	311.3	50.6	865	0.32	33,309	1824	3505
01-13_35_sp1	0.0451	0.0028	0.3166	0.0239	0.7554	284.3	17.2	279.2	18.4	237.0	114.6	366	0.44	7208	384	961
01-14_4_sp1 R*	0.0458	0.0019	0.3229	0.0143	0.8876	288.9	11.7	284.1	11.0	244.8	47.2	1553	0.03	12,530	655	150
01-14_12_sp1 R*	0.0483	0.0016	0.3416	0.0144	0.8169	304.2	9.6	298.4	10.9	253.1	56.2	704	0.20	11,699	622	752
01-14_16_sp2 R*	0.0478	0.0022	0.3460	0.0167	0.9580	301.3	13.5	301.7	12.6	305.3	31.6	3592	0.27	2815	162	265
01-14_23_sp1 R*	0.0452	0.0022	0.3198	0.0201	0.7804	284.8	13.8	281.8	15.5	256.6	90.4	1370	0.30	1513	93	159
01-14_13_sp1 R	0.0141	0.0013	0.1036	0.0262	0.4371	90.3	8.3	100.1	24.2	339.6	518.0	5675	0.22	64	18	39
01-14_26_sp1 R	0.0387	0.0018	0.2749	0.0175	0.6931	244.9	11.0	246.6	13.9	262.9	105.4	3970	0.02	904	61	36
01-14_18_sp1 R*	0.0448	0.0016	0.3174	0.0142	0.6982	282.2	9.7	279.9	10.9	260.3	74.0	300	0.39	8594	455	1058
01-14_20_sp1 C	0.0730	0.0031	0.5575	0.0268	0.9030	454.1	18.9	449.9	17.5	428.6	46.0	615	0.13	20,432	1154	878
01-14_1_sp1 C	0.0553	0.0036	0.4224	0.0297	0.9532	346.9	22.2	357.8	21.2	428.6	47.6	881	0.16	33,360	1877	2090
01-14_2_sp2 C	0.0751	0.0028	0.5719	0.0251	0.8320	467.0	16.7	459.2	16.2	420.7	54.4	441	0.06	10,772	607	226
01-14_11_sp1 C	0.0517	0.0025	0.3710	0.0202	0.9288	325.2	15.1	320.4	15.0	285.2	46.6	676	0.01	11,025	586	49

01-14_17_sp1 C	0.0621	0.0021	0.4694	0.0179	0.7949	388.7	12.6	390.8	12.4	403.1	52.4	506	0.06	18,863	1041	319
01-14_16_sp1 C*	0.0441	0.0021	0.3147	0.0219	0.8412	278.0	13.0	277.8	16.9	276.6	89.4	229	0.52	8027	435	1434
01-14_4_sp2 C	0.0540	0.0027	0.4112	0.0227	0.9388	338.8	16.7	349.7	16.3	423.2	42.6	371	0.24	19,148	1065	1523
01-14_5_sp1 C	0.0701	0.0028	0.5690	0.0240	0.8705	437.0	17.1	457.3	15.5	560.8	46.0	390	0.06	20,521	1212	803
01-6_1_sp1*	0.0482	0.0019	0.3463	0.0275	0.6789	303.3	11.6	301.9	20.7	291.6	137.5	246	0.67	22,677	1193	5454
01-6_2_sp1*	0.0466	0.0013	0.3328	0.0142	0.4950	293.7	8.3	291.7	10.8	275.4	86.7	398	0.93	11,463	621	3370
01-6_3_sp1*	0.0483	0.0015	0.3537	0.0167	0.6883	304.0	9.1	307.5	12.5	334.3	77.7	344	0.93	18,038	923	5286
01-6_4_sp1*	0.0488	0.0012	0.3542	0.0127	0.8405	307.1	7.5	307.9	9.5	313.8	45.5	620	0.88	100,680	5320	27780
01-6_5_sp1*	0.0474	0.0017	0.3322	0.0246	0.3745	298.6	10.6	291.3	18.7	233.0	159.7	207	1.02	10,512	596	3455
01-6_6_sp1*	0.0497	0.0021	0.3628	0.0245	0.7654	312.7	13.1	314.3	18.2	326.2	100.3	172	1.08	27,308	1426	9892
01-6_7_sp1	0.0413	0.0020	0.2951	0.0177	0.8536	261.0	12.4	262.6	13.9	277.1	71.8	290	0.97	49,062	2411	13910
01-6_9_sp1*	0.0483	0.0016	0.3392	0.0347	0.5560	303.9	9.7	296.5	26.3	238.8	204.1	137	0.90	3673	210	1006
01-6_12_sp1*	0.0507	0.0013	0.3639	0.0176	0.7672	319.1	8.2	315.1	13.1	286.2	75.3	418	0.92	10,962	592	3193
01-6_16_sp1*	0.0465	0.0020	0.3377	0.0175	0.7931	293.2	12.2	295.4	13.3	312.7	71.8	311	0.98	28,144	1512	8409
01-6_18_sp1*	0.0485	0.0011	0.3460	0.0139	0.5864	305.6	6.8	301.7	10.5	271.7	74.5	510	0.93	9383	493	2685
01-6_22_sp1	0.0439	0.0019	0.3072	0.0191	0.6245	276.7	11.9	272.0	14.8	231.4	112.6	194	0.92	8586	443	2361
01-6_24_sp1	0.0454	0.0025	0.3028	0.0378	0.5659	285.9	15.6	268.6	29.4	119.9	245.0	129	0.91	2001	107	600
01-6_25_sp1	0.0516	0.0021	0.3582	0.0233	0.6979	324.3	13.0	310.9	17.4	211.4	108.4	281	0.88	5699	298	1621
01-6_30_sp1	0.0435	0.0023	0.3060	0.0224	0.6974	274.6	14.3	271.1	17.5	240.8	121.3	167	1.08	5468	295	1745
01-16_1_sp1*	0.0493	0.0021	0.3445	0.0308	0.6810	310.4	13.0	300.6	23.2	224.7	156.7	378	0.35	1753	99	217
01-16_2_sp1*	0.0474	0.0019	0.3247	0.0312	0.6660	298.3	11.7	285.5	23.9	182.3	176.2	324	0.35	2914	158	351
01-16_5_sp1*	0.0489	0.0019	0.3404	0.0296	0.5665	307.6	11.6	297.5	22.4	218.8	167.9	481	0.55	901	57	182
01-16_25_sp1*	0.0458	0.0016	0.3299	0.0151	0.7963	288.8	10.0	289.5	11.5	295.5	63.1	648	0.56	15,208	812	2647
01-16_29_sp1*	0.0481	0.0014	0.3454	0.0218	0.5820	302.8	8.7	301.3	16.4	289.7	118.1	398	0.31	2523	142	276
01-16_30_sp1*	0.0475	0.0012	0.3447	0.0277	0.6069	299.2	7.2	300.7	20.9	312.6	155.2	399	0.47	3418	186	508
01-16_31_sp1*	0.0509	0.0021	0.3767	0.0452	0.7117	319.8	12.7	324.6	33.3	358.8	215.1	369	0.35	1321	82	166
01-16_33_sp1*	0.0486	0.0025	0.3540	0.0258	0.7412	305.6	15.3	307.8	19.3	323.9	111.1	437	0.35	2959	157	320
01-16_35_sp1*	0.0487	0.0020	0.3547	0.0332	0.7126	306.8	12.0	308.3	24.9	319.3	160.9	492	0.35	2282	135	281
01-16_38_sp1*	0.0493	0.0018	0.3609	0.0264	0.7371	310.0	10.9	312.9	19.7	334.8	119.3	508	0.42	3400	188	460
02-9_19_sp1 R*	0.0500	0.0012	0.3610	0.0097	0.9265	314.4	7.7	312.9	7.3	302.2	23.1	5149	0.03	1263	77	39
02-9_25_sp1 R*	0.0501	0.0010	0.3648	0.0082	0.8643	314.9	6.2	315.8	6.1	322.1	25.8	2226	0.07	5480	291	127
02-9_27_sp1 R*	0.0489	0.0021	0.3487	0.0158	0.9591	307.6	12.8	303.7	11.9	273.8	29.4	10,015	0.02	635	46	38
02-9_11_sp2 C*	0.0492	0.0013	0.3575	0.0152	0.7332	309.3	7.9	310.4	11.3	318.2	66.6	1451	0.14	3748	204	170
02-9_13_sp1 C	0.0884	0.0018	0.8725	0.0235	0.7220	546.3	10.8	636.9	12.8	973.0	38.1	642	0.02	2854	210	37
02-9_20_sp1 C	0.0708	0.0027	0.4957	0.0676	0.4339	440.8	16.5	408.8	45.9	231.7	287.3	172	0.25	1673	105	188
02-9_7_sp2 C	0.0536	0.0011	0.4002	0.0094	0.9284	336.5	7.0	341.8	6.8	378.1	19.6	5079	0.06	6118	327	111
02-9_1_sp1 C	0.0734	0.0026	0.5650	0.0467	0.6523	456.4	15.4	454.8	30.3	446.5	145.3	325	0.09	2551	156	97
02-9_10_sp1 C	0.0715	0.0028	0.5628	0.0350	0.8150	445.3	16.8	453.4	22.8	494.6	83.5	226	0.11	9349	544	394
02-9_27_sp2 C	0.0701	0.0026	0.5552	0.0223	0.9296	437.0	15.9	448.4	14.6	507.1	32.6	1062	0.28	17,277	1008	1745
02-9_25_sp2 C	0.0532	0.0014	0.3789	0.0218	0.5388	334.4	8.8	326.2	16.0	268.4	111.4	602	0.03	4588	253	54
02-9_29_sp1 C	0.0562	0.0037	0.4294	0.0377	0.8281	352.5	22.7	362.8	26.8	428.9	110.8	478	0.23	1251	74	105
02-9_40_sp1 C	0.0943	0.0021	0.8026	0.0335	0.6615	580.8	12.2	598.3	18.9	665.3	68.1	1147	0.58	1768	115	333

R=magmatic rim, C=inherited core. * Denotes analyses used in age regressions.

[a] Analysis label denotes sample#_grain#_spot#.

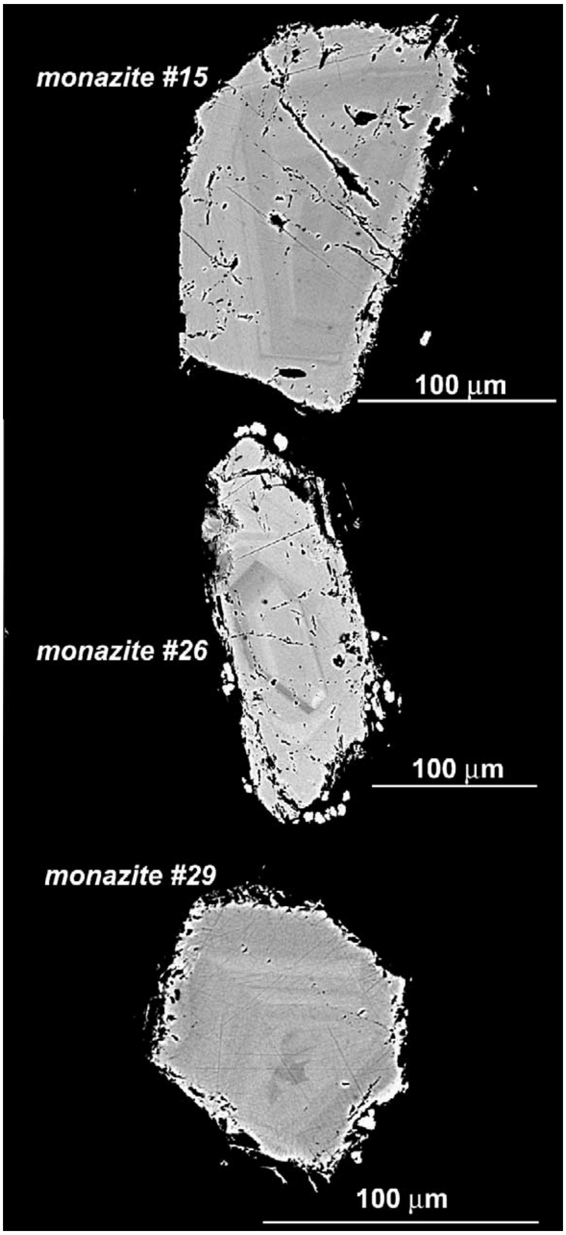

Fig. 8. BSE images of representative monazite grains from the Koprivshtitsa two-mica granite (02-9). Grains typically show faint oscillatory zoning indicative of magmatic growth.

around their edges that are a few micrometers thick at most. The thin rims make analysis very difficult, and the resulting confidence in the ages is somewhat diminished, primarily due to the small number of quality analyses that we were able to obtain. Inherited cores display a wide variety of zoning characteristics. Some clearly have a magmatic origin and display euhedral, concentric oscillatory zoning. The ages of such zones, however, are highly variable, and they do not represent new growth in the magma chamber of these rocks, but rather the magmatic textures were preserved from an older event. A few zones that are clearly inherited cores based upon textural evidence yield ages that are similar to those of the magmatic rims. We interpret these as completely reset during the magmatic event. They are therefore recording the magmatic age and not inherited ages, and were included in the age calculations. Several analysis spots clearly straddled the rims and inherited cores (after viewing analytical spots in BSE images and reflected light) and yielded older, discordant ages, which we justifiably discarded as mixed analyses.

For the Koprivshtitsa granite (BG02-9), we obtained 8 analyses of magmatic rims and 10 analyses of inherited cores. However, the small size of the magmatic rims resulted in most analyses overlapping core and rim material, and these were discarded. One analysis (11_sp2) from a center portion of a grain is indistinguishable from the remaining analyses of magmatic rims and was therefore included in the age calculation; additionally, the grain has a very high aspect ratio (Fig. 4). The analyses yield a concordia age of 312.0±5.4 Ma

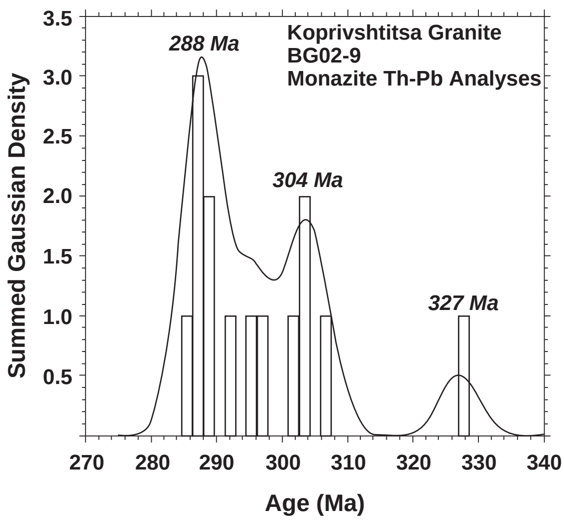

Fig. 9. Combined probability plot and histogram of $^{208}Pb^{*}/^{232}Th$ monazite age data for the Koprivshtitsa granite (02-9). Zircon age of ~312 Ma is not reflected in the monazite data.

Table 2
HR-SIMS Th–Pb monazite data for analyzed spots

Analysis	Isotopic ratios		Calculated ages		Th/U	$^{208}Pb/^{204}Pb$
	$^{208}Pb*/^{232}Th$	2σ	$^{208}Pb*/^{232}Th$	2σ		
02-9_1_sp1	0.01631	0.00030	327.1	5.9	31	6107
02-9_2_sp1	0.01529	0.00028	306.8	5.5	30	11,266
02-9_5_sp1	0.01504	0.00028	301.7	5.5	20	3414
02-9_7_sp1	0.01516	0.00027	304.2	5.4	16	10,785
02-9_9_sp1	0.01473	0.00027	295.5	5.3	11	1581
02-9_10_sp1	0.01458	0.00027	292.5	5.4	9	4750
02-9_11_sp1	0.01512	0.00028	303.3	5.7	44	10,841
02-9_13_sp1	0.01441	0.00026	289.2	5.2	79	10,372
02-9_15_sp1	0.01480	0.00027	297.0	5.4	12	5669
02-9_18_sp1	0.01420	0.00026	285.0	5.2	22	4815
02-9_21_sp1	0.01435	0.00029	287.9	5.8	16	10,619
02-9_26_sp1	0.01437	0.00026	288.3	5.1	25	7964
02-9_29_sp1	0.01430	0.00026	287.0	5.1	58	11,697
02-9_34_sp1	0.01431	0.00026	287.2	5.2	4	8076
01-14_7_sp1	0.01387	0.00025	278.4	4.9	16	10,717

(MSWD equiv.=1.5, MSWD conc.=1.7, n=4; Fig. 5E). The probability plot along concordia also yields a similar peak at 314 Ma (Fig. 6E).

We obtained seven analyses of magmatic rims and eight analyses of inherited cores on zircons from the Strelcha pluton (BG01-14). Two analyses of magmatic rims (13_sp1, 26_sp1) are significantly younger than the rest of the population, and BSE images indicate that the beam overlapped with cracks in the grains. These two analyses are therefore interpreted to represent partial Pb loss. One analysis of core material yields an age similar to the remaining five analyses of rim material. The combined analyses yield a concordia age of 289.5±7.8 Ma (MSWD equiv.=2.5, MSWD conc.=1.8, n=6; Fig. 5F). Removing the analysis of core material does not significantly affect the calculated age or the statistical parameters. The probability plot along concordia yields two peaks at 282 and 302 Ma, indicating excess scatter in the data consistent with the high MSWD of equivalence (Fig. 6F), but the age cannot be further resolved without additional data.

As mentioned previously, zircons from both samples of two-mica granites are ~80–90% xenocrystic. The number of analyses of cores is not large, especially given the statistical considerations of Dodson et al. (1988) and Sircombe (2000), but does allow some comments to be made. Both samples have apparent ages that range from ~300–400 Ma; these may be partially reset by magmatism and geologically meaningless, or some may reflect the age of metamorphism of the basement rocks. Both samples yield a subpopulation of cores with ages at ~450 Ma. Additionally, the Koprivshtitsa granite yielded two discordant analyses that are Neoproterozoic ($^{207}Pb*/^{206}Pb*$ ages of ~665 and 975 Ma), and the Strelcha granite also yielded a discordant analysis with a Neoproterozoic $^{207}Pb*/^{206}Pb*$ age ~560 Ma (Fig. 7). These two granites were therefore likely derived from a common source region containing both Early Paleozoic and Neoproterozoic age components.

4.2.2.2. Monazite ages. Monazite grains show faint zoning in BSE, but most are consistent with growth from magma (Fig. 8). The Strelcha pluton (BG01-14) did not yield enough monazite to be dated properly; a single analysis is 278.4±4.9 Ma, which is slightly younger than, but similar to, the age obtained from the zircon data. Monazite from the Koprivshtitsa granite (BG02-9) yields a range of ages from ~307 Ma to ~285 Ma, with one older outlying analysis at 327.1±5.9 Ma (Fig. 9). This analysis is somewhat older than the crystallization age determined by the zircon data and may be an inherited age. The probability plot of the monazite Th–Pb data yields two younger, distinct peaks at ~304 and ~288 Ma. The BSE images, however, give little indication that a

Table 3
Preferred magmatic ages

Sample name (number)	Magmatic age (Ma)	Inheritance (Ma)	Prior geochronology
Balkan Terrane			
San Nikola granite (01-1)	311.9±4.1	None	None
Petrohan granodiorite (01-6)	304.6±4.0	None	None
Sredna Gora Terrane			
Biotite granites			
Smilovene granite (01-13)	304.1±5.5	None	342±27 (Rb–Sr)[a]
Hisara granite (01-16)	303.5±3.3	None	337±14 (Rb–Sr)[a]
Two-mica granites			
Koprivshtitsa granite (02-9)	312.0±5.4	~450, ~665–975	301±7 (Rb–Sr)[b]
Strelcha granite (01-14)	289.5±7.8	~450, ~560	238±37 (Rb–Sr)[b]

[a] Moorbath and Zagorchev (1983).
[b] Zagorchev and Moorbath (1986).

mixed population is present. Neither of these ages is similar to the zircon magmatic age (312.0±5.4 Ma), but both are similar to ages of other intrusions in the immediate area, specifically the Smilovene (BG01-13, 304.1±5.5 Ma) and the Strelcha (BG01-14, 289.5±7.8 Ma) plutons. We interpret the monazite ages as partially reset during the intrusion of nearby plutons. Townsend et al. (2001) discussed in detail the resetting of magmatic monazite by intrusion of a younger, nearby pluton, and similar processes may be causing younger ages in the monazite of this study.

5. Discussion

5.1. Timing of terrane accretion in southeastern Europe

The timing of the amalgamation of the various terranes of the Balkan Peninsula is still not clearly known, although the Balkan, Sredna Gora and possibly parts of the Rhodope, were likely attached to southern Europe during the Variscan Orogeny (Haydoutov and Yanev, 1997; Yanev, 2000). The identification of similar granitoids in both the Balkan and Sredna Gora Terranes provides a possible correlation. In addition to their similar chemistry and mineralogy, the zircon data of calc-alkaline granitoids from both terranes are very similar. The ages of the four samples span a narrow range from 311.9±4.1 Ma to 303.5±3.3 Ma. These similarities suggest a genetic connection between these granites that are separated by a terrane boundary (reactivated as an Alpine fault), which in turn implies that the docking of these two terranes occurred prior to ~312 Ma, during Early Late Carboniferous time. It cannot be completely ruled out that these suites of granites were generated in separate geographical areas and the terranes amalgamated later, but the striking similarities between the granites, combined with a lack of deformational structures in them, more likely indicate a common source region and that terrane juxtaposition had already occurred.

5.2. Petrogenetic model for the Variscan granitoids of Bulgaria

The new HR-SIMS U–Pb zircon ages constrain the timing of magmatism in central Bulgaria to an interval of less than ~25 million years, rather than the ~100 million years suggested by the Rb–Sr results (Moorbath and Zagorchev, 1983; Zagorchev and Moorbath, 1986). None of the granites yield HR-SIMS zircon U–Pb ages as old as ~340 Ma or as young as ~240 Ma. Rather than different styles of magmatism emplaced in separate intervals, the new data suggest that the two suites were generated and emplaced at roughly the same time, with most of the ages clustering ~305 Ma. The ages are similar to that recently obtained for the related Vejen pluton located within the Balkan Terrane (Kamenov et al., 2002). The Koprivshtitsa granite (BG02-9, 312.0±5.4, suite 2A) is among the oldest ages determined in this study and is apparently older than the Smilovene granite of the first suite (BG01-13, 304.1±5.5 Ma) just to the south, contrary to previous studies that considered the first suite as the earliest phase of magmatism (Zagorchev et al., 1973; Moorbath and Zagorchev, 1983; Zagorchev and Moorbath, 1986). Although the two-mica leucocratic Strelcha pluton (BG01-14, 289.5±7.8 Ma, suite 2B) appears to be somewhat younger than the other granites (~315–305 Ma), there is greater uncertainty in the age and the true age may be very similar. Regardless, it is clearly much older than the Triassic age (~240 Ma) suggested by the Rb–Sr data. The ages for the two samples of leucogranites are distinct, but it is not clear whether these different ages are truly representative of the entire series of two-mica granites or if the two subsuites overlap in age.

Although geochronological data now indicate that the two suites of intrusions are roughly coeval, geochemical data clearly show that the two suites are not genetically related. The rocks of the first suite are similar in mineralogy and geochemistry to calc-alkaline granites commonly found near convergent margins, and which are particularly common in the North American Cordillera (Patiño Douce, 1999). Continued differentiation of rocks such as these may lead to highly evolved leucocratic melts that can form two-mica granites (Miller, 1985), possibly like the two-mica granites studied here. However, the high Sr (300–400 ppm), low K_2O/Na_2O values (~0.6–1.0), moderate LREE concentrations (~50–100× chondrite) and moderate Eu anomalies of these two-mica granites indicate that they are not highly evolved melts produced by fractionation of a significant amount of feldspar. Additionally, their initial Sr isotopic ratios and zircon inheritance patterns are significantly different from the first suite, precluding the leucogranites from being derived by partial melting or continued differentiation of the first suite. Rather, the two suites of granites must have been derived from different source regions. The first suite of intrusions, with their calc-alkaline geochemistry and related gabbroic to dioritic rocks, are consistent with an influx of mafic material from the mantle, and various assimilation, remelting, and fractional crystallization processes to produce the more felsic varieties. Based upon initial Sr isotopic ratios, the second suite requires a source that is either older or has a distinctly higher Rb/Sr ratio; either is more crustal like. The most obvious sources for the second suite are the metasedimentary mica-schists and metapsammites that make up the basement of the Sredna Gora Terrane.

The paucity of zircon inheritance in the first suite, contrasted with the overwhelming amount of inheritance in the second suite, likely indicates that zircon saturation was vastly different in their respective source regions during melting. In their survey of zircon saturation temperatures for a variety of granitoids, Miller et al. (2003) found that granitoids fall into a bi-modal distribution, whereby those with abundant zircon inheritance have generally lower T_{Zr} by ~70 °C compared with granitoids that lack inheritance (mean T_{Zr} of 837 °C for inheritance poor vs. 766 °C for inheritance rich granitoids). Furthermore, high amounts of inheritance typically lead to an overestimation of T_{Zr}, while in samples with no inheritance T_{Zr} must be considered minimum temperatures of melt generation. Miller et al. (2003) interpreted this bi-modal distribution of temperatures as resulting from different melt generating mechanisms. High temperature granitoids may have been formed by standard melting mechanisms such as influx of mantle heat and dehydration of hydrous mafic phases (i.e., biotite and amphibole), while lower temperature granites likely require an influx of water-rich fluid into high-grade rocks or breakdown of abundant muscovite (Miller et al., 2003). Assuming that the findings of Miller et al. (2003) are applicable to the granitoid suites investigated here, the two suites were likely generated at different temperatures, and therefore by different melt generating mechanisms. Zircon saturation temperatures calculated for these two suites are anomalously low for granitic rocks (690–740 °C and 600–690 °C, respectively), but do imply that the inheritance-poor granitoids are higher temperature melts than the leucogranites, as expected from the clear differences in zircon xenocryst preservation.

Thrusting of the Sredna Gora Terrane over the Balkan Terrane may have liberated a water-rich fluid from the unmetamorphosed sedimentary rocks and greenschist facies metamafic rocks of the Balkan Terrane. Migration of this fluid into the overlying Sredna Gora Terrane, which was metamorphosed to high grades at ~335 Ma (Carrigan unpub. data in prep), may have triggered H_2O-fluxed melting to generate low temperature granitic melts. The geochemistry of the two-mica granites requires in this kind of melting scenario that their source regions contain plagioclase, K-feldspar and quartz (Patiño Douce, 1999), such as metapsammitic rocks common in the Sredna Gora Terrane. Furthermore, the high Sr concentrations are not consistent with melting solely of pelitic material.

The association of the volcanic equivalents interlayered with continental molasse deposits has led previous workers to regard the Variscan granitoids as collisional related (Haydoutov, 1991). Our model, which requires influx of heat from the mantle to generate the first suite, and influx of water into high-grade, metapsammites to generate the second suite, is compatible with post-collisional generation of these intrusions, but the presence of gabbroic rocks and calc-alkaline diorites and granodiorites also suggests continued subduction of ocean crust underneath the southern margin of Europe after the collision of the Balkan and Sredna Gora Terranes during the Variscan Orogeny.

5.3. Comparison to granitoids across the Variscan belt

Post-collisional granitoids are particularly common in Variscan massifs across Europe. Finger et al. (1997) divided granitoids of central Europe into five suites that are thought to differ in age, source region, and tectonic setting. The southern portion of the Bohemian Massif (Fig. 1) is intruded by the South Bohemian Batholith, which is a composite body made of several granitic intrusions of a variety of ages, the most significant of which is the Weinsberg granitoid (Finger et al., 1997; Klötzli et al., 2001). Pb evaporation data and isotope dilution, thermal ionization mass spectrometry (ID-TIMS) U–Pb data of Klötzli et al. (2001) suggest ages of 345±5 Ma, but also indicate significant amounts of inheritance of Cambrian and Paleoproterozoic age. The magmatic age, however, is older than the high-grade metamorphism of the country rocks at 339.8±2.6 Ma (Kröner et al., 2000, zircon U–Pb HR-SIMS). HR-SIMS dating of zircon from samples of the Weinsberg granitoid by Finger et al. (2003) yielded crystallization ages of 322±4 Ma and inherited ages of ~2 Ga and ~450 Ma, and no evidence of ~345 Ma or Cambrian ages. It seems likely that the Pb evaporation and ID-TIMS U–Pb data of Klötzli et al. (2001) represent a mixed population of ages. Additional zircon U–Pb ID-TIMS ages of the South Bohemian Batholith also yield ages from 330.7±2 Ma to 323±1 Ma in the Weinsberg granite, and similar ages for diorites from 327.4±0.8 Ma to 316±1 Ma (Gerdes et al., 2003). Monazite U–Pb ID-TIMS analyses for fine-grained granites yielded ages of 316±1 Ma and 315±1 Ma (Gerdes et al., 2003).

Farther to the north, the Central Bohemian Batholith is also a composite intrusion consisting of multiple phases of magmatism (e.g., Janoušek et al., 2000). Calc-alkaline intrusions of the Sázava suite dated by zircon U–Pb ID-TIMS yield an upper intercept age of 354.1±3.5 Ma (Janoušek and Gerdes, 2003; Janoušek et al., this volume). Zircon fractions from the Tábor intrusion (Èertovo bøemeno suite) yield a younger age of 336.6±1.0 Ma (Janoušek and Gerdes, 2003). Similar durbachite rocks farther east yielded nearly identical ages (also zircon ID-TIMS) of 335.2±0.54 Ma (Kotkova et al., 2003). Still farther north, two monzonite intrusions in the Northern Bohemian Massif (Meissen Massif) yielded U–Pb zircon HR-SIMS ages of 330.5±4.6 Ma and 326.5±6.3 Ma, with Mesoproterozoic inherited cores ~1.2–1.8 Ga (Nasdala et al., 1999). Ages for two younger granitoids (304±14 Ma) by zircon Pb evaporation methods were reported by Kröner et al. (1994) for rocks also in the northern Bohemian Massif. However, without supporting U data, these ages must be treated with caution. Younger ages, however, appear to be present within the Harz Mountain Range (Fig. 1), where Baumann et al. (1991) obtained ID-TIMS U–Pb zircon ages for the Harzburg gabbronorite (294±1 Ma; 293±2 Ma) and the Brocken granite (~300 Ma).

Volcanic rocks within the southern Black Forest Massif (Fig. 1), interpreted as emplaced in an intracontinental setting (based upon the high-K character of rhyolites near the top of the succession), yield an age of 340±2 Ma (Schaltegger, 1997, 2000). Granitoids also occur as both pre- and post-deformational intrusions in the southern Black Forest, and three post-deformational granitoids are well dated at ~333 Ma (332±3 Ma, 333±2 Ma and 334±3 Ma; Schaltegger, 2000). Two monazite fractions from a strongly deformed granite yield an age of 334±2 Ma, indistinguishable from the ages of the undeformed granitoids (Schaltegger, 2000). A granite porphyry dike, cutting the undeformed granitoids, also yields an equivalent age of 332_{-4}^{+2} Ma, and a caldera-filling rhyolite was also dated at 333±3 Ma (Schaltegger, 2000).

Rocks in the southern portion of the Vosges Massif (Fig. 1) appear similar and correlative to those of the Black Forest Massif. U–Pb zircon ID-TIMS ages for volcanic rocks are somewhat problematic, as some samples are plagued by inheritance, but two samples yielded concordant ages of 345±2 Ma (lower unit) and 340±2 Ma (upper unit; Schaltegger et al., 1996). The volcano-sedimentary rocks are bounded by high-K granitic and dioritic to monzonitic intrusions that yield U–Pb zircon and titanite ID-TIMS ages ~340 Ma (342±1 Ma, 340_{-2}^{+4} Ma, 340±1 Ma and 339.5±2.5 Ma; Schaltegger et al., 1996). Younger ages are also present as a high-K, mafic durbachite, well dated at 332±3 Ma (Schulmann et al., 2002), and later granite at 325.8±4.8 Ma (Schaltegger et al., 1999).

Granitoids of the northern portions of both the Vosges and Black Forest Massifs consist of diorites, granodiorites, and calc-alkaline granites. K–Ar and $^{40}Ar/^{39}Ar$ ages from biotite and hornblende for these rocks cluster ~330–325 Ma (331.0±3.0 Ma, 331±12 Ma, 330.5±3.0 Ma, 328±6 Ma, 326±11 Ma, 325±12 Ma and 331±11 Ma; Edel et al., 1986; Hess et al., 1995; Altherr et al., 2000, and references therein). High-K granites also occur and are possibly correlative to high-K granites in the southern Vosges with ages of ~340 Ma (Schulmann et al., 2002). Strongly peraluminous granites comprise the final phase of granitic magmatism. Pb evaporation age for a representative of the youngest leucogranites (Kagenfels) yielded an age of 331±5 Ma, suggesting that all suites of magma were emplaced in a fairly short time interval (Hess et al., 1995), but Pb evaporation data for leucogranites may not be reliable indicators of crystallization ages.

In the central Iberian Massif (Fig. 1), Bea et al. (1999) described magmatism present in the Avila Batholith and generated Rb–Sr isochron ages for representative intrusions. These intrusions consist of volumetrically small calc-alkaline mafic rocks, voluminous granitoids and lamprophyric dike swarms. Samples of the calc-alkaline mafic rocks yielded an Rb–Sr age of 340±18 Ma. Granodiorites yielded ages of 327±8 Ma and 317±13 Ma, monzogranites and granodiorites yielded ages of 306±8 Ma and 310±9 Ma, two-mica granites yielded ages of 295±13 Ma and 297±26 Ma, and leucogranites yielded ages of 344±5 Ma and 305±16 Ma (Bea et al., 1999). Since the leucogranites typically intrude the first suite of granodiorites, the older age ~344 Ma appears to be suspect. The lamprophyric dikes yielded an age of 283±30 Ma.

Farther north within the Iberian Massif, Fernández-Suárez et al. (2000) obtained U–Pb ID-TIMS ages on syn- and post-tectonic intrusions. Syntectonic intrusions yielded upper intercept ages of 323_{-5}^{+9} Ma, 317_{-5}^{+9} Ma and 313±2 Ma (Fernández-Suárez et al., 2000). Monazite analyses in these samples predominantly yield younger ages of 295±2 Ma and 293±2 Ma (Fernández-Suárez et al., 2000), and the similarity of the ages to the younger post-tectonic intrusions suggests that the monazites were reset by the younger events. The ages for the post-tectonic intrusions are ~295–290 Ma (295±3 Ma, 292±3 Ma, 289±3 Ma, 295±2 Ma and 286±2 Ma; Fernández-Suárez et al., 2000), but as only a few fractions are concordant, the ages are predominantly upper intercept ages. Zircons from a hornblendite intrusion yielded a similar upper intercept age of 293_{-2}^{+3} Ma (Fernández-Suárez et al., 2000).

Dias et al. (1998) also presented zircon and monazite U–Pb ID-TIMS ages for granitoids from the central Iberian zone of northern Portugal. The oldest ages cluster ~320–313 Ma (319.0±3.6 Ma, 316.1±2.5 Ma, 314.2±2.2 Ma, and 313.1±2.1 Ma; Dias et al., 1998). A second stage of emplacement is represented by ages ranging from ~310–308 Ma (310.7±5.1 Ma, 309.3±2.6 Ma, 309.2±0.6 Ma, 306.8±3.5 Ma, and 306.4±2.1 Ma; Dias et al., 1998). The youngest intrusions yield ages in the range ~295–280 Ma (296.7±7.0 Ma, 290.1±2.5 Ma, and 279.5±4.6 Ma; Dias et al., 1998). Similar ages were obtained in a zircon and monazite U–Pb ID-TIMS study by Azevedo et al. (2003) where syntectonic monzogranites and two-mica leucogranites yielded ages of ~311 Ma, 308 Ma, and 306 Ma (no errors given).

Within the Alpine region, several massifs of Variscan granitoids are exposed (Fig. 1). For the Aar Batholith, U–Pb ID-TIMS ages for both zircon and titanite of high-K shoshonitic rocks are predominantly concordant and in the range ~330–335 Ma, with a mean zircon age of 334±2.5 Ma (Schaltegger and Corfu, 1992). Diorites and granites are also present and yield younger ages ~310–308 Ma (308±2 Ma, 310±3 Ma, and 309±2 Ma); a still younger suite of granites and granodiorites yields ages of 299±2 Ma and 297±2 Ma (Schaltegger and Corfu, 1992). These ages are in agreement with others discussed by Schaltegger (1994). Farther east, calc-alkaline granodiorites of the Bernina Batholith also yield U–Pb ID-TIMS ages ~325–340 Ma (332±15 Ma, 338±18 Ma, 324±12 Ma, 338±9 Ma, and 332±18 Ma), while younger alkaline granites and rhyolites yield ages ~290–300 Ma (295±12 Ma, 288±7 Ma, and 292±6 Ma; von Quadt et al., 1994). Unfortunately, these data contain almost no concordant fractions and the errors are quite large, but the data do suggest two age populations of intrusive activity. Still farther east, Eichhorn et al. (2000) obtained HR-SIMS U–Pb zircon data for numerous intrusions in the Tauern window. Earlier granites yield ages ~340 Ma (343±6 Ma, 342±5 Ma, and 340±4 Ma), while younger granitoids and volcanics yield ages ~295–300 Ma (300±5 Ma, 299±4 Ma, and 296±4 Ma; Eichhorn et al., 2000). Granitoids within the Carpathians farther east are poorly known, much like the Balkans, but many investigated samples from the Velká Fatra mountains yield zircon ages ~310 Ma (Poller et al., 2005).

From the available data, granitoids in the Bohemian Massif, Black Forest Massif, Vosges Massif, and the intra-Alpine massifs record an older episode of Variscan granitoid magmatism ~325–340 Ma. Younger granitoids ~310–295 Ma may also be present within these massifs, and their ages are well established in the intra-Alpine massifs. To the west in the Iberian Massif, granitoids appear to be predominantly younger, with the oldest ages ~320 Ma. Younger granitoids ~310–295 Ma appear to be predominant. The eastern portion of the orogen within Bulgaria and surrounding areas does not appear to record an older phase of Variscan magmatism ~340–325 Ma; rather, the ages are predominantly ~315–290 Ma and are more similar to those from the Iberian Massif and the younger ages of the intra-Alpine massifs, than to the predominantly older ages in the central portions of the orogen. Nearly all of these intrusions are considered post-collisional and generated after the main compressional and high-grade metamorphic events of the Variscan Orogeny. As such, comparison of these intrusive rocks may yield insights into the large-scale processes across the orogen. Preservation and completeness of the data obscure the reliability of any interpretations, but one possibility is that the trend of ages indicates that the culmination of collision and orogenic processes causing partial crustal melting between adjacent crustal blocks was completed in the central portion of the orogen prior to the western, eastern, and more southerly areas of the orogen.

Acknowledgements

We thank Kevin McKeegan and Marty Grove for their assistance in obtaining high quality isotopic results on the Cameca IMS 1270 at UCLA. We gratefully acknowledge the UCLA staff for providing the monazite standards. The University of California, Los Angeles IMP laboratory is partially funded by a grant from the National Science Foundation Instrument and Facilities program. Zeb Page and Kate Griffin assisted in operating the Cameca IMS 1270. Carl Henderson provided valuable assistance in operating the electron microbeam instruments at the University of Michigan. The Cameca SX-100 was funded by NSF grant EAR-99-11352 and the Hitachi scanning electron microscope by NSF grant EAR-96-28196. Funding for this work came from NSF grant INT-0227687 to SBM and University of Michigan, Department of Geological Sciences Turner grants to CWC. Eric J. Essene and Calvin F. Miller provided helpful comments on an earlier version of the manuscript. Urs Schaltegger, Axel Gerdes and J.P. Burg are acknowledged for their critical reviews, and we thank U. Schaltegger for his editorial handling of the manuscript. The paper further benefited from discussions with Rebecca A. Lange and Ben A. van der Pluijm. The manuscript comprises one chapter of the doctoral dissertation of CWC at the University of Michigan.

References

Altherr, R., Holl, A., Hegner, E., Langer, C., Kreuzer, H., 2000. High-potassium, calc-alkaline I-type plutonism in the European Variscides: northern Vosges (France) and northern Schwarzwald (Germany). Lithos 50, 51–73.

Arnaudov, V., Amov, B., Baldjieva, Ts., Pavlova, M., 1990. Tertiary magmatic pegmatites in the Central Rhodope crystalline complex. Uranium–lead zircon dating. Geol. Balc. 20 (6), 25–32.

Azevedo, M.R., Valle Aguado, B., Schaltegger, U., Nolan, J., Medina, J., Martins, M.E., 2003. U–Pb zircon and monazite geochronology of Variscan magmatism related to syn-convergence extension in central northern Portugal. J. Czech Geol. Soc. 48, 16.

Baumann, A., Grauert, B., Mecklenburg, S., Vinx, R., 1991. Isotopic age determinations of crystalline rocks of the Upper Harz Mountains, Germany. Geol. Rundsch. (Int. J. Earth Sci.) 80, 669–690.

Bea, F., Montero, P., Molina, J.F., 1999. Mafic precursors, peraluminous granitoids, and late lamprophyres in the avila batholith: a model for the generation of Variscan batholiths in Iberia. J. Geol. 107, 399–419.

Best, M.G., Christiansen, E.H., 2001. Igneous Petrology. Oxford Blackwell Science. 480 pp.

Boyadjiev, S., 1991. Comparative petrologic-geochemical characterization of the pre-Mesozoic granitoids of the Sredna Gora zone. Geol. Balc. 21 (3), 35–74.

Burg, J.-P., Ivanov, Z., Ricou, L.-E., Dimov, D., Klain, L., 1990. Implications of shear-sense criteria for the tectonic evolution of the Central Rhodope massif, southern Bulgaria. Geology 18, 451–454.

Carrigan, C.W., Miller, C.F., Fullagar, P.D., Bream, B.R., Hatcher Jr., R.D., Coath, C.D., 2003a. Ion microprobe age and geochemistry of southern Appalachian basement, with implications for Proterozoic and Paleozoic reconstructions. Precambrian Res. 120, 1–36.

Carrigan, C.W., Mukasa, S.B., Haydoutov, I., Kolcheva, K., 2003b. Ion microprobe U–Pb zircon ages of pre-Alpine rocks in the Balkan, Sredna Gora, and Rhodope Terranes of Bulgaira: constraints on Neoproterozoic and Variscan tectonic evolution. J. Czech Geol. Soc. 48, 32–33.

Cherneva, Z., Ovtcharova, M., von Quadt, A., Kolcheva, K., Stancheva, E., Sarov, S., Peytcheva, I., 2002. Monazite and zircon U–Pb ages of migmatites from the Arda River Valley, Central Rhodopian Dome, Bulgaria. In: Dabovcski, C., Ivanov, I. (Eds.), Modern Problems of the Bulgarian Geological Society, Annual Sci. Conf. Abstr., pp. 20–22.

Dias, G., Leterrier, J., Mendes, A., Simões, P.P., Bertrand, J.M., 1998. U–Pb zircon and monazite geochronology of post-collisional Hercynian granitoids from the Central Iberian Zone (northern Portugal). Lithos 45, 349–369.

Dimitrova, E., Belmustakova, K., 1982a. Eclogite relicts in the Sredna Gora crystalline schist complex. Geol. Balc. 12 (1), 115–120.

Dimitrova, E., Belmustakova, K., 1982b. Metamorphic facies in the crystalline schists of Sredna Gora, Ikhtiman. Geohim. Mineral. Petrol. 16, 61–67.

Dodson, M.H., Compston, W., Williams, I.S., Wilson, J.F., 1988. A search for ancient detrital zircons in Zimbabwean sediments. J. Geol. Soc. (Lond.) 145, 977–983.

Edel, J.B., Montigney, R., Royer, J.Y., Thuizat, R., Troland, F., 1986. Paleomagnetic investigations and K–Ar dating on the Variscan plutonic massif of the Camp du Feu and its volcanic-sedimentary environment, northern Vosges, France. Tectonophysics 122, 165–185.

Eichhorn, R., Loth, G., Höll, R., Finger, F., Schermaier, A., Kennedy, A., 2000. Multistage Variscan magmatism in the central Tauern Window (Austria) unveiled by U/Pb SHRIMP zircon data. Contrib. Mineral. Petrol. 139, 418–435.

Fernández-Suárez, J., Dunning, G.R., Jenner, G.A., Gutiérrez-Alonso, G., 2000. Variscan collisional magmatism and deformation in NW Iberia: constraints from U–Pb geochronology of granitoids. J. Geol. Soc. (Lond.) 157, 565–576.

Finger, F., Roberts, M.P., Haunschmid, B., Schermaier, A., Steyrer, H.P., 1997. Variscan granitoids of central Europe: their typology, potential sources and tectonothermal relations. Mineral. Petrol. 61, 67–96.

Finger, F., Doblmayr, P., Friedl, G., Gerdes, A., Krenn, E., Von Quadt, A., 2003. Petrology of the Weinsberg granite in the South Bohemian Batholith: new data from the mafic end members. J. Czech Geol. Soc. 48, 46–47.

Gerdes, A., Friedl, G., Parrish, R.R., Finger, F., 2003. High-resolution geochronology of Variscan granite emplacement—the South Bohemian Batholith. J. Czech Geol. Soc. 48, 53–54.

Hanchar, J.M., Miller, C.F., 1993. Zircon zonation patterns as revealed by cathodoluminescence and backscattered electron images; implications for interpretation of complex crustal histories. Chem. Geol. 110, 1–13.

Harrison, T.M., McKeegan, K.D., LeFort, P., 1995. Detection of inherited monazite in the Manaslu leucogranite by $^{208}Pb/^{232}Th$ ion microprobe dating: crystallization age and tectonic implications. Earth Planet. Sci. Lett. 133, 271–282.

Harrison, T.M., Grove, M., McKeegan, K.D., Coath, C.D., Lovera, O.M., LeFort, P., 1999. Origin and episodic emplacement of the Manaslu intrusive complex, Central Himalaya. J. Petrol. 40, 3–19.

Haydoutov, I., 1989. Precambrian ophiolites, Cambrian island arc, and Variscan suture in the South Carpathian-Balkan region. Geology 17, 905–908.

Haydoutov, I., 1991. The Thracian Hercynian suture and the related magmatism. Geotecton. Tectonophysics Geodyn., Sofia 23, 3–25 (in Bulgarian with English summary).

Haydoutov, I., Yanev, S., 1997. The Protomoesian microcontinent of the Balkan Peninsula—a peri-Gondwanaland piece. Tectonophysics 272, 303–313.

Hess, J.C., Lippolt, H.J., Kober, B., 1995. The age of the Kagenfels granite (northern Vosges) and its bearing on the intrusion scheme of late Variscan granitoids. Geol. Rundsch. (Int. J. Earth Sci.) 84, 568–577.

Janoušek, V., Gerdes, A., 2003. Timing the magmatic activity within the Central Bohemian Pluton, Czech Republic: conventional U–Pb ages for the Sázava and Tabor intrusions and their geotectonic significance. J. Czech Geol. Soc. 48, 70–71.

Janoušek, V., Bowes, D.R., Rogers, G., Farrow, C.M., Jelínek, E., 2000. Modeling diverse processes in the petrogenesis of a composite batholith: the Central Bohemian Pluton, Central European Hercynides. J. Petrol. 41, 511–543.

Janoušek, V., Braithwaite, C.J.R., Bowes, D.R., Gerdes, A., this volume. Magma mixing in the genesis of Hercynian calc-alkaline granitoids: an integrated petrographic and geochemical study of the Sázava intrusion, Central Bohemian Pluton, Czech Republic.

Kalenic, M., 1966. First find of Lower Cambrian in Eastern Serbia–Southern Carpathian mountains. Bulg. Geol. Soc. Rev. (Sofia) 27, 216–220 (in Bulgarian with English summary).

Kalvacheva, R., 1986. Acritarch stratigraphy of the Ordovician System in Bulgaria. Final Field Meeting. International Geological Correlation Programme, Project 5, Sardinia, pp. 38–43.

Kamenov, B., von Quadt, A., Peytcheva, I., 2002. New insight into petrology, geochemistry, and dating of the Vejen Pluton, Bulgaria. Geochem. Mineral. Petrol. 39, 3–26.

Klötzli, U.S., Koller, F., Scharbert, S., Höck, V., 2001. Cadomian lower-crustal contributions to Variscan granite petrogenesis (South Bohemian Pluton, Austria): constraints from zircon typology and geochronology, whole-rock, and feldspar Pb–Sr isotope systematics. J. Petrol. 42, 1621–1642.

Kotkova, J., Schaltegger, U., Leichmann, J., 2003. 338–335 Ma old intrusions in the E Bohemian Massif—a relic of the orogen-wide durbachitic magmatism in European Variscides. J. Czech Geol. Soc. 48, 80–81.

Kozhoukharov, D., 1987. The Rhodopian Supergroup in the Avren Syncline, Eastern Rhodopes. Geol. Balc. 17 (4), 21–40 (in Russian).

Kozhoukharova, E., 1985. Origin and structural position of the serpentinized ultrabasic rocks from the Precambrian ophiolite association in Rhodope Massif III, Development stages and age of the ophiolite association. Geol. Balc. 15 (5), 53–69 (in Russian).

Kozhoukharova, E., 1996. New data for the geological position of the Precambrian ophiolitic association in the Rhodope Massif. C. R. Acad. Bulg. Sci. 49 (1), 57–60.

Kröner, A., Hegner, E., Hammer, J., Haase, G., Bielicki, K.-H., Krauss, M., Eidam, J., 1994. Geochronology and Nd–Sr systematics of Lusatian granitoids: significance for the evolution of the Variscan orogen in east-central Europe. Geol. Rundsch. (Int. J. Earth Sci.) 83, 357–376.

Kröner, A., O'Brien, P.J., Nemchin, A.A., Pidgeon, R.T., 2000. Zircon ages for high-pressure granulites from South Bohemia, Czech Republic, and their connection to the Carboniferous high temperature processes. Contrib. Mineral. Petrol. 138, 127–142.

Liati, A., Gebauer, D., 1999. Constraining the prograde and retrograde *P–T–t* path of Eocene HP rocks by SHRIMP dating of different zircon domains: inferred rates of heating, burial, cooling and exhumation for central Rhodope, northern Greece. Contrib. Mineral. Petrol. 135, 340–354.

Liati, A., Mposkos, E., 1990. Evolution of the eclogites in the Rhodope zone of northern Greece. Lithos 25, 89–99.

Lilov, P., 1981. Potassium–argon dating of the Struma Diorite formation north of the town of Stanke Dimitrov. Geol. Balc. 11 (2), 27–31.

Ludwig, K.R., 1991. ISOPLOT—a plotting and regression program for radiogenic-isotope data. Reson, VA: US Geological Survey OF91-0445.

Ludwig, K.R., 1998. On the treatment of concordant uranium–lead ages. Geochim. Cosmochim. Acta 62, 665–676.

Matte, P., 1986. Tectonics and plate tectonics model for the Variscan belt of Europe. Tectonophysics 126, 329–374.

Matte, P., 1991. Accretionary history and crustal evolution of the Variscan belt in western Europe. Tectonophysics 196, 309–337.

McKerrow, W.S., MacNiocaill, C., Ahlberg, P.E., Clayton, G., Cleal, C.J., Eagar, R.M.C., 2000. The Late Palaeozoic relations between Gondwana and Laurussia. In: Franke, W., Haak, V., Oncken, O., Tanner, D. (Eds.), Orogenic processes: quantification and modelling in the Variscan belt, Geological Society, London, Special Publications, vol. 179, pp. 9–20.

Miller, C.F., 1985. Are strongly peraluminous magmas derived from pelitic sedimentary sources? J. Geol. 93, 673–689.

Miller, C.F., Hanchar, J.M., Wooden, J.L., Bennett, V.C., Harrison, T.M., Wark, D.A., Foster, D.A., 1992. Source region of a granite batholith; evidence from lower crustal xenoliths and inherited accessory minerals. Trans. R. Soc. Edinb. Earth Sci. 83, 49–62.

Miller, C.F., Hatcher Jr., R.D., Ayers, J.C., Coath, C.D., Harrison, T.M., 2000. Age and zircon inheritance of eastern Blue Ridge plutons, southwestern North Carolina and northeastern Georgia, with implications for magma history and evolution of the southern Appalachian orogen. Am. J. Sci. 300, 142–172.

Miller, C.F., Meschter McDowell, S., Mapes, R.W., 2003. Hot and cold granites? Implications of zircon saturation temperatures and preservation of inheritance. Geology 31, 529–532.

Moorbath, S., Zagorchev, I., 1983. Rubidium–strontium isotopic data on the age of the first granitoid complex (Smilovene and Hisar plutons) in Sastinska Sredna Gora. Geol. Balc. 13 (3), 3–14.

Mposkos, E., 1989. High-pressure metamorphism in gneisses and pelitic schists in the east Rhodope zone (N. Greece). Mineral. Petrol. 41, 25–39.

Muttoni, G., Gaetani, M., Budurov, K., Zagorchev, I., Trifonova, E., Ivanova, D., Petrounova, L., Lowrie, W., 2000. Middle Triassic paleomagnetic data from northern Bulgaria; constraints on Tethyan magnetostratigraphy and paleogeography. Palaeogeogr. Palaeoclimatol. Palaeoecol. 160, 223–237.

Muttoni, G., Kent, D.V., Garzanti, E., Brack, P., Abrahamsen, N., Gaetani, M., 2003. Early Permian Pangea 'B' to Late Permian Pangea 'A'. Earth Planet. Sci. Lett. 215, 379–394.

Nance, R.D., Murphy, J.B., 1994. Contrasting basement isotopic signatures and the palinspastic restoration of peripheral orogens; example from the Neoproterozoic Avalonian–Cadomian belt. Geology 22, 617–620.

Nasdala, L., Wenzel, T., Pidgeon, R.T., Kronz, A., 1999. Internal structures and dating of complex zircons from Meissen Massif monzonites, Saxony. Chem. Geol. 156, 331–341.

Paces, J.B., Miller Jr, J.D., 1993. Precise U–Pb ages of Duluth complex and related mafic intrusions, northeastern Minnesota: geochronological insights to physical, petrogenetic, paleomagnetic, and tectonomagmatic processes associated with the 1.1 Ga mid-continent rift system. J. Geophys. Res. 98 (B8), 13997–14013.

Papanikolaou, D., Panagopoulos, A., 1981. On the structural style of southern Rhodope, Greece. Geol. Balc. 1113, 13–22.

Paterson, B.A., Stephens, W.E., Herd, D.A., 1989. Zoning in granitoid accessory minerals as revealed by backscattered electron imagery. Mineral. Mag. 53, 55–61.

Patiño Douce, A.E., 1999. What do experiments tell us about relative contributions of crust and mantle to the origin of granitic magmas? In: Castro, A., Fernandez, C., Vigneresse, J.L. (Eds.), Understanding Granites; Integrating New and Classical Techniques, Geol. Soc. (London) Special Publications, vol. 168, pp. 55–75.

Pearce, J.A., Harris, N.B.W., Tindle, A.G., 1984. Trace element discrimination diagrams for the tectonic interpretation of granitic rocks. J. Petrol. 25, 956–983.

Peytcheva, I., von Quadt, A., 1995. U–Pb zircon dating of metagranites from Byala-reka region in the east Rhodopes, Bulgaria. Proceedings of the XV Congress of the Carpatho-Balcan Geological Association, Sept., 1995, Athens, Geol. Soc. Greece Special Publication, vol. 4, 2, pp. 637–642.

Peytcheva, I., Salnikova, E., Kosticin, K., Ovtcharova, M., Sarov, S., 2000. Metagranites from the Madan-Davidkovo dome, Central Rhodopes: U–Pb and Sr–Rb protholite and metamorphism dating. ABCD-Geode 67.

Poller, U., Kohut, M., Anders, B., Todt, W., 2005. Multistage geochronological evolution of the Velká Fatra Mountains – a combined TIMS and ion-microprobe study on zircons. Lithos 82, 113–124. (this volume).

Quidelleur, X., Grove, M., Lovera, O.M., Harrison, T.M., Yin, A., 1997. Thermal evolution and slip history of the Renbu Zedong thrust, southeastern Tibet. J. Geophys. Res. 102 (B2), 2659–2679.

Ruseva, M., 1978. On a petrochemical feature of the granitoids between Panagurishte and Koprivshtica (Sredna Gora). Annu. Super. Mines Geol., Sofia 22 (2), 131–141 (in Bulgarian).

Sãndulescu, M., 1994. Overview of Romanian geology. Rom. J. Tecton. Reg. Geol. 75 (Suppl. 2), 3–17.

Savov, I., Ryan, J., Haydoutov, I., Schijf, J., 2001. Late Precambrian Balkan–Carpathian ophiolite; a slice of the Pan-African ocean crust? Geochemical and tectonic insights from the Tcherni Vrah and Deli Jovan massifs, Bulgaria and Serbia. J. Volcanol. Geotherm. Res. 110, 299–318.

Schaltegger, U., 1994. Unravelling the pre-Mesozoic history of Aar and Gotthard massifs (Central Alps) by isotopic dating—a review. Schweiz. Mineral. Petrogr. Mitt. 74, 41–51.

Schaltegger, U., 1997. Magma pulses in the central Variscan belt: episodic melt generation and emplacement during lithospheric thinning. Terra Nova 9, 242–245.

Schaltegger, U., 2000. U–Pb geochronology of the Southern Black Forest Batholith (central Variscan belt): timing of exhumation and granite emplacement. Int. J. Earth Sci. 88, 814–828.

Schaltegger, U., Corfu, F., 1992. The age and source of Late Hercynian magmatism in the central Alps: evidence from precise U–Pb ages and initial Hf isotopes. Contrib. Mineral. Petrol. 111, 329–344.

Schaltegger, U., Schneider, J.-L., Maurin, J.-C., Corfu, F., 1996. Precise U–Pb chronometry of 345–340 Ma old magmatism related to syn-convergence extension in the southern Vosges (central Variscan belt). Earth Planet. Sci. Lett. 144, 403–419.

Schaltegger, U., Fanning, C.M., Günther, D., Maurin, J.C., Schulmann, K., Gebauer, D., 1999. Growth, annealing and recrystallization of zircon and preservation of monazite in high-grade metamorphism: conventional and in-situ U–Pb isotope, cathodoluminescence and microchemical evidence. Contrib. Mineral. Petrol. 134, 186–201.

Schmitz, M.D., Bowring, S.A., Ireland, T.R., 2003. Evaluation of Duluth Complex anorthositic series (AS3) zircon as a U–Pb geochronological standard: new high-precision isotope dilution thermal ionization mass spectrometry results. Geochim. Cosmochim. Acta 67, 3665–3672.

Schulmann, K., Schaltegger, U., Jezek, J., Thompson, A.B., Edel, J.-B., 2002. Rapid burial and exhumation during orogeny: thickening and synconvergent exhumation of thermally weakened and thinned crust (Variscan orogen in western Europe). Am. J. Sci. 302, 856–879.

Seghedi, A., Oaie, G., Rădan, S., 1999. Late Proterozoic–Early Cambrian turbidites from Central Dobrogea—provenance and significance. Rom. J. Tecton. Reg. Geol. 77 (Suppl. 1).

Şengör, A.M.C., 1987. Tectonics of the Tethysides: orogenic collage development in a collisional setting. Annu. Rev. Earth Planet. Sci. 15, 213–244.

Sircombe, K.N., 2000. Quantitative comparison of large sets of geochronological data using multivariate analysis; a provenance study example from Australia. Geochim. Cosmochim. Acta 64, 1593–1616.

Stacey, J.S., Kramers, J.D., 1975. Approximation of terrestrial lead isotope evolution by a two-stage model. Earth Planet. Sci. Lett. 26, 207–211.

Stampfli, G.M., Borel, G.D., 2002. A plate tectonic model for the Paleozoic and Mesozoic constrained by dynamic plate boundaries and restored synthetic oceanic isochrons. Earth Planet. Sci. Lett. 196, 17–33.

Tait, J.A., Bachtadse, V., Franke, W., Soffel, H.C., 1997. Geodynamic evolution of the European Variscan fold belt; palaeomagnetic and geological constraints. Geol. Rundsch. (Int. J. Earth Sci.) 86, 585–598.

Tait, J., Schtz, M., Bachtadse, V., Soffel, H., 2000. Palaeomagnetism and Palaeozoic palaeogeography of Gondwana and European terranes. In: Franke, W., Haak, V., Oncken, O., Tanner, D. (Eds.), Orogenic Processes: Quantification and Modelling in the Variscan Belt, Geological Society, London, Special Publications, vol. 179, pp. 21–34.

Townsend, K.J., Miller, C.F., D'Andrea, J.L., Ayers, J.C., Harrison, T.M., Coath, C.D., 2001. Low temperature replacement of monazite in the Ireteba Granite, southern Nevada; geochronological implications. Chem. Geol. 172, 95–112.

Van der Voo, R., 1988. Paleozoic paleogeography of North America, Gondwana, and intervening displaced terranes: comparisons of paleomagnetism with paleoclimatology and biogeographical patterns. Geol. Soc. Am. Bull. 100, 311–324.

Vavra, G., 1990. On the kinematics of zircon growth and its petrogenetic significance; a cathodoluminescence study. Contrib. Mineral. Petrol. 106, 90–99.

von Quadt, A., Grünenfelder, M., Büchi, H., 1994. U–Pb zircon ages from igneous rocks of the Bernina nappe system (Grisons, Switzerland). Schweiz. Mineral. Petrogr. Mitt. 74, 373–382.

von Quadt, A., Peytcheva, I., Haydoutov, I., 1998. U–Pb zircon dating of Tcherny Vrach Metagabbro, the West Balkan, Bulgaria. C. R. Acad. Bulg. Sci. 51 (1–2), 81–84.

Watson, E.B., Harrison, T.M., 1983. Zircon saturation revisited; temperature and composition effects in a variety of crustal magma types. Earth Planet. Sci. Lett. 64, 295–304.

Wawrzenitz, N., Mposkos, E., 1997. First evidence for Lower Cretaceous HP/HT-metamorphism in the eastern Rhodope, North Aegean Region, North-East Greece. Eur. J. Mineral. 9, 659–664.

Wiedenbeck, M., Allé, P., Corfu, F., Griffin, W.L., Meier, M., Oberli, F., von Quadt, A., Roddick, J.C., Spiegel, W., 1995. Three natural zircon standards for U–Th–Pb, Lu–Hf, trace element and REE analyses. Geostand. Newsl. 19, 1–23.

Winchester, J.A., Pharaoh, T.C., Verniers, J., 2002. Palaeozoic amalgamation of central Europe: an introduction and synthesis of new results from recent geological and geophysical investigations. In: Winchester, J.A., Pharaoh, T.C., Verniers, J. (Eds.), Palaeozoic Amalgamation of Central Europe, Geological Society, London, Special Publications, vol. 201, pp. 1–18.

Windley, B.F., 1995. The Evolving Continents, 3rd edition. John Wiley & Sons, Ltd. 544 pp.

Yanev, S., 2000. Palaeozoic terranes of the Balkan Peninsula in the framework of Pangea assembly. Palaeogeogr. Palaeoclimatol. Palaeoecol. 161, 151–177.

Zagorchev, I., Moorbath, S., 1986. Rb–Sr dating of the granitoid magmatism in Sastinska Sredna Gora. Rev. Bulg. Geol. Soc. 47 (3), 62–68.

Zagorchev, I., Dabovski, H., Chunev, D., 1973. On the tectonics of the western part of the Sredna Gora crystalline block (Sredna Gora proper). Rev. Bulg. Geol. Soc. 34 (1), 1–10.

Ziegler, P.A., 1986. Geodynmaic model for the Paleozoic crustal consolidation of western and central Europe. Tectonophysics 126, 303–328.